BT-1033

Motions of a Payload on a Tethered, Aerodynamic-Shape Balloon Using Various Cable Lengths

Air Force Cambridge Research Labs.

Don E. Jackson; Catherine B. Rice

17 Mar 1975

AFCRL-TR-75-0148
INSTRUMENTATION PAPERS, NO. 229

Motions of a Payload on a Tethered, Aerodynamic-Shape Balloon Using Various Cable Lengths

DON E. JACKSON, Capt, USAF
CATHERINE B. RICE

17 March 1975

AEROSPACE INSTRUMENTATION LABORATORY PROJECT 6665
AIR FORCE CAMBRIDGE RESEARCH LABORATORIES
HANSCOM AFB, MASSACHUSETTS 01731

AIR FORCE SYSTEMS COMMAND, USAF

Unclassified

SECURITY CLASSIFICATION OF THIS PAGE (When Data Entered)

REPORT DOCUMENTATION PAGE		READ INSTRUCTIONS BEFORE COMPLETING FORM
1. REPORT NUMBER AFCRL-TR-75-0148	2. GOVT ACCESSION NO.	3. RECIPIENT'S CATALOG NUMBER
4. TITLE (and Subtitle) MOTIONS OF A PAYLOAD ON A TETHERED, AERODYNAMIC-SHAPE BALLOON USING VARIOUS CABLE LENGTHS		5. TYPE OF REPORT & PERIOD COVERED Scientific. Interim. 6. PERFORMING ORG. REPORT NUMBER IP No. 229
7. AUTHOR(s) Don E. Jackson, Capt USAF Catherine B. Rice		8. CONTRACT OR GRANT NUMBER(s)
9. PERFORMING ORGANIZATION NAME AND ADDRESS Air Force Cambridge Research Laboratories (LCB) Hanscom AFB Massachusetts 01731		10. PROGRAM ELEMENT, PROJECT, TASK AREA & WORK UNIT NUMBERS 62101F 66650901
11. CONTROLLING OFFICE NAME AND ADDRESS Air Force Cambridge Research Laboratories (LCB) Hanscom AFB Massachusetts 01731		12. REPORT DATE 17 March 1975 13. NUMBER OF PAGES 60
14. MONITORING AGENCY NAME & ADDRESS(if different from Controlling Office)		15. SECURITY CLASS. (of this report) Unclassified 15a. DECLASSIFICATION/DOWNGRADING SCHEDULE

16. DISTRIBUTION STATEMENT (of this Report)

Approved for public release; distribution unlimited.

17. DISTRIBUTION STATEMENT (of the abstract entered in Block 20, if different from Report)

18. SUPPLEMENTARY NOTES

19. KEY WORDS (Continue on reverse side if necessary and identify by block number)

Balloon
Tethered balloon

20. ABSTRACT (Continue on reverse side if necessary and identify by block number)

A series of flight tests of a classic British barrage (kite) balloon, 2.83×10^3 m^3 in size, were made at White Sands Missile Range. The tests were made in a variety of wind conditions and tether lengths. The report presents the motions of a payload suspended beneath the balloon as measured by ground-based cinetheodolites and balloon-borne sensors. Included in the data are horizontal and vertical trajectories, maximum displacement, pitch and roll angles, ground speed, and acceleration.

DD FORM 1 JAN 73 1473 EDITION OF 1 NOV 65 IS OBSOLETE

Unclassified

SECURITY CLASSIFICATION OF THIS PAGE (When Data Entered)

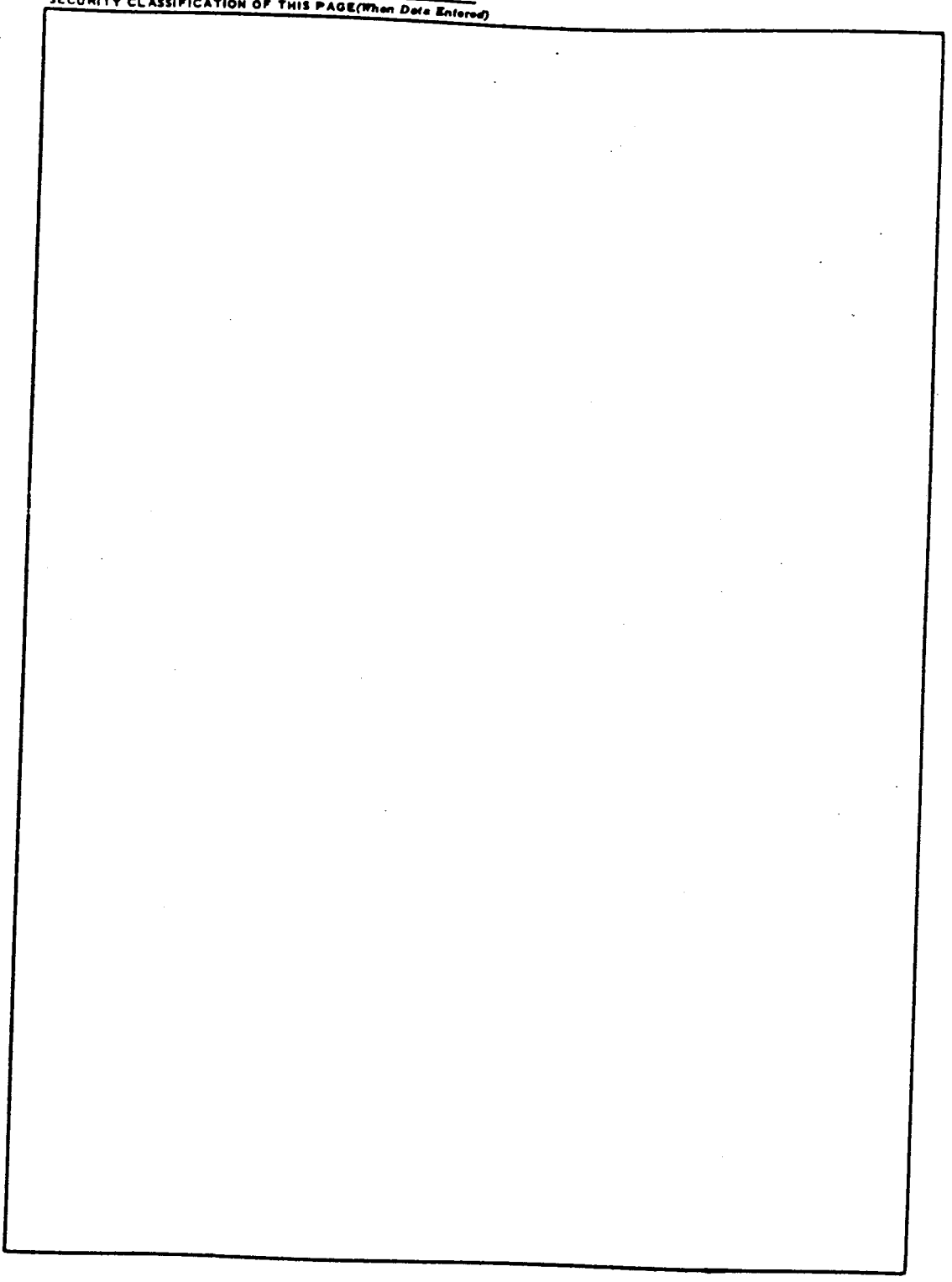

Contents

Contents

Illustrations

Illustrations

Tables

Motions of a Payload on a Tethered, Aerodynamic-Shape Balloon Using Various Cable Lengths

1. INTRODUCTION

In a typical year, the USAF tethered-balloon schedule might include advanced parachute development tests, atmospheric sampling, boundary-layer measurements, communications experiments, and drop tests of space components.* The slow, very limited motions of a well-designed tethered balloon system do not affect most of the testing activities that require a "tower" or platform at heights up to 6 km MSL. But if the payload will employ pointing controls, or an exceptionally sensitive mechanical device, then the motions of the balloon system must be considered in designing the instrumentation and in planning the test procedure. To provide this information, AFCRL has been conducting experimental stability studies of various tethered systems which are currently in use at the USA tethered balloon test facilities at Holloman AFB and White Sands Missile Range (WSMR), New Mexico.

The 2.83×10^3 m^3 balloon flown at Fair Site on WSMR has a classic British kite shape (Figure 1). This design has been completely modernized, using neoprene-coated nylon balloon fabric, a high-speed winch, lightweight, high strength NOLARO tether cable, and state-of-the-art electronics for telemetry and

(Received for publication 14 March 1975)

*The Aerospace Instrumentation Laboratory, Air Force Cambridge Research Laboratories (AFCRL) conducts the USAF balloon activities at permanent sites in New Mexico and at temporary sites using mobile equipment wherever the experiment is required.

Figure 1. The 2.83×10^3 m^3 A-Shape Balloon at Fair Site

command-control of the experimental operations and safety functions. This balloon can support 2.2×10^3 N payloads at 3.6 km elevation above ground at Fair Site (elevation 1.44 km MSL), and somewhat larger loads at lower altitudes. Dimensions, position of the center of gravity, center of buoyancy, and rigging confluence point are shown in Appendix A.

This report presents the results of eighteen 20-min observations of the motions of a payload at the confluence point of the 2.83×10^3 m^3 British kite balloon. These tests were made during a period of seven days in April 1973 at Fair Site, New Mexico. The balloon was flown on a 2.74 km, 5/8-in. diam NOLARO cable in average winds up to 15 m/sec; and on a 1.52 km cable of the same diameter in average winds up to 9.3 m/sec. There also were two tests using an 0.305 km cable in winds below 5.1 m/sec.

The position of the payload in Cartesian coordinates, and its velocity and acceleration relative to ground for 1-sec intervals were determined by the WSMR cinetheodolite system. The optical target was a black and white pattern painted on the payload. The payload was mounted on a horizontal load bar, one end of which was rigidly attached to the quadplate at the confluence point, and the other end, through cables to load patches on the balloon (Figures 1 and 2).

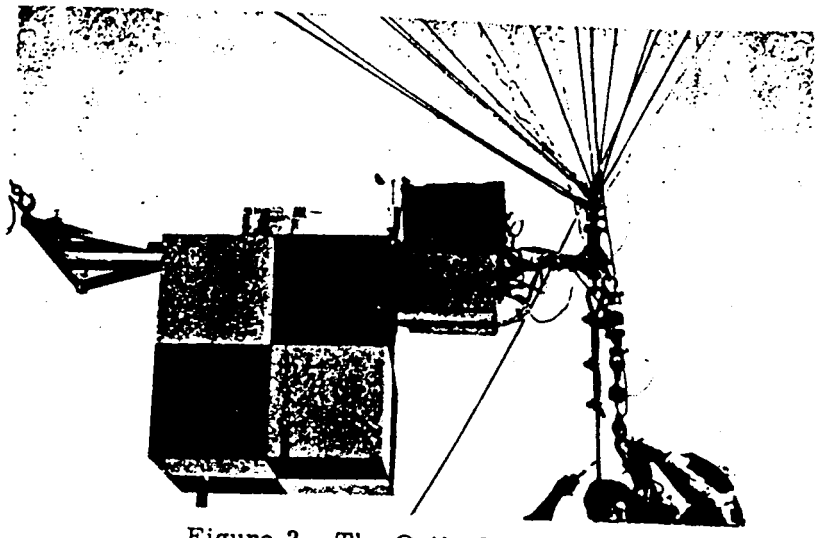

Figure 2. The Optical Target

Profiles of wind velocity from surface level to the balloon altitude were derived from observations of PIlot BALloons (PIBALS) which were released as close in time as possible to the start and end of each test. The balloon-borne anemometer wind data, payload pitch and roll angles, and cable tension at the confluence point were recorded by continuous telemetry.

Trajectories in the horizontal and vertical planes are presented for several typical flights. In some cases the horizontal motion has also been converted to displacements in directions parallel and normal to the PIBAL-determined wind direction at balloon altitude. For each flight test, the maximum values of displacements, pitch and roll angles, ground speed and acceleration are tabulated together with the range in values of cable tension at the confluence point, the extremes, and average values of relative wind speed (anemometer), and the displacement of the balloon "equilibrium position" from the winch. (The equilibrium position is the estimated location on the ground above which the balloon tended to hover or to wander.) Empirical relationships among some of these parameters are derived and the relevance of these results to flight planning is briefly discussed.

2. FLIGHT RESULTS

2.1 Flights on 2.74 km Cable (Nominal Length)

Results for the five flights on 2.67, 2.68, and 2.74 km lengths of cable are summarized in Tables 1(a) and 1(b).* The "typical maximum ground speed" is

*Each tabulation of results is presented in two tables, one using metric, and one, British units.

Table 1(a). (English Units)
Flights on 9000-Ft Cable (Nominal Length)

Flight No. / Start Time MST	PIBAL Wind at Balloon Alt.		Equil. Distance	Range in Alt. (ft)	Avg. Alt. AGL	Max. Wander	Max. Tang. Acceleration	Cable Tension (lb)	
	Speed (kt)	Dir. (deg)	d (ft)	During 20 Min	(ft)	(ft)		Min. / Max.	Typical
11R3 / 11:00	18	267	960	42	9290	390	< 0.1 G	2700 / 3100	2900
12R1 / 11:00	12 17	250 250	910 1130	75	9021	1010	< 0.1 G	2550 / 2650	2600
12R2 / 12:00	15 16	245 250	1420	177	8957	2200	0.1 G	2100 / 3200	2500
13R1 / 14:00 cable 8800 ft.	26	200	3420	364	8044	1720	0.1 G	1950 / 3550	2900
13R2 / 15:00 cable 8750 ft.	27 24	200 225	3250 2800	613	8240	1760 2000	0.1 G	2200 / 3850	3000
17R1 / 13:00	17	260	1700	209	8800	1620	< 0.1 G	2200 / 2700	2450
16R3 / 13:00 cable 8000 ft 7000 ft	18 (reeled in due to clouds)	190		32 228	7788 6871		0.1 G	1800 / 3700	2600

Table 1(a). (Metric Units)
Flights on 2.74 km Cable (Nominal Length)

Flight No. / Start Time MST	PIBAL Wind at Balloon Alt.		Equil. Distance	Range in Alt. (m)	Avg. Alt. AGL	Max. Wander	Max. Tang. Acceleration	Cable Tension (N)	
	Speed m/sec	Dir. (deg)	d (m)	During 20 Min	(m)	(m)	m/sec^2	Min. / Max.	Typical
11R3 / 11:00	9.3	267	293	13	2832	119	< 0.1	120×10^2 / 138×10^2	129×10^2
12R1 / 11:00	6.2* 8.7	250 250	277* 344	23	2750	308	< 0.1	114×10^2 / 118×10^2	116×10^2
12R2 / 12:00	7.7* 8.2	245 250	433	54	2730	671	0.1	93.6×10^2 / 143×10^2	111×10^2
13R1 / 14:00 cable 2682 m	13.4	200	1042	111	2452	824	0.1	86.9×10^2 / 158×10^2	129×10^2
13R2 / 15:00 cable 2667 m	13.9* 12.3	200 225	991* 853	187	2512	536 610	0.1	98.0×10^2 / 172×10^2	134×10^2
17R1 / 13:00	8.7	260	518	64	2682	494	< 0.1	98.0×10^2 / 120×10^2	109×10^2
16R3 / 13:00	9.3	190		98 70	2374 2094		0.1	80.2×10^2 / 165×10^2	116×10^2
cable 8000 ft 7000 ft (reeled in due to clouds)									

*Data at beginning and end of flight.

Table 1(b). (English Units)
Flights on 9000-ft Cable (Cont)

Flight No.	Maximum Ground Speed During a Typical Excursion (ft/sec)	Maximum Ground Speed During the Test (ft/sec)	Anemometer Wind (kt) Range	Anemometer Wind (kt) Average	Maximum Pitch Angle (degrees)	Maximum Roll Angle (degrees)
11R3	2	6	14-19	15	<1.2	<1.8
12R1	4	7	No wind data		<5	<1.8
12R2	15	28	No wind data		18.2 (typical, max. was 7.2)	16
13R1		30	<8-43.5	27	12	7.2
13R2		31	<8-43	27	24.5	7.2
17R1	5	24		18	No Data	
16R3	15	30	<8-27		12	9

Table 1(b). (Metric Units)
Flights on 2.74 km Cable (Cont)

Flight No.	Maximum Ground Speed During a Typical Excursion (m/sec)	Maximum Ground Speed During the Test (m/sec)	Anemometer Wind (m/sec) Range	Anemometer Wind (m/sec) Average	Maximum Pitch Angle (degrees)	Maximum Roll Angle (degrees)
11R3	0.61	1.8	7.2 - 9.8	7.7	1.2	1.8
12R1	1.2	2.1	No Wind Data		5	1.8
12R2	4.6	8.5	No Wind Data		18.2 (typical max. 7.2)	16
13R1		9.1	4.1 - 22.4	13.9	12	7.2
13R2		9.5	4.1 - 22.1	13.9	24.5	7.2
17R1	1.5	7.3		9.3	No Data	
16R3	4.6	9.1	4.1 - 13.9		12°	9

the approximate maximum speed attained during a typical excursion of the balloon. The maximum tangential speed is the highest value recorded during the 20-min test.

2.1.1 FLIGHT 11R3

Figure 3 is the horizontal trajectory of the balloon for Flight 11R3, when the PIBAL-detected wind was 9.3 m/sec. The target altitude and displacement in the directions approximately parallel and transverse to the PIBAL wind direction versus time, and the wind profile acting along the cable are also plotted in Figure 3.

The transverse displacement curve suggests a 480-sec periodicity, with the curve between 220 and 700 sec fairly well duplicated between 700 and 1180 sec. Longitudinal displacements tend to correlate with the very small simultaneous changes in altitude. The maximum range in altitude was 12.8 m in 20 min. During most of this flight the tangential ground speed was 0.30 m/sec or less; in one 5-sec interval, 240 to 245 sec, this speed peaked at 1.8 m/sec. Acceleration was less than 0.55 m/sec^2. Barely discernible changes in pitch (1.2°) and roll (1.8°) and a gradual 1.78×10^3-N increase in the otherwise steady tension occurred at the times noted on Figure 3. The relative wind speed at the target was 7.2 to 9.8 m/sec.

2.1.2 FLIGHT 12R1

In 6.2 to 8.8 m/sec wind, Flight 12R1 had an almost linear horizontal trajectory (Figure 4) which, like Flight 11R3, might also be expected to reveal simple modes of orthogonal motions relative to the wind direction. Here the balloon appears to have been displaced by an obliquely directed, slow gust from which it made a highly damped recovery. Maximum displacement in altitude was 23 m and maximum tangential speed was 2.1 m/sec. There was no measurable rolling motion (less than 1.8°) and no pitching until the last 3.5 min of flight when the target gently pitched toward ±4.8° about every 10 sec. Cable tension at the confluence point was steady except during the same pitching interval, when it varied ±222 N from 1.16×10^4 N. The slant range of the target from the winch was highest during that interval.

2.1.3 FLIGHT 12R2

More complex motions and greater displacements and speeds occurred in the gustier winds during the remaining flights on the 2.74 km tether (nominal length). On Flight 12R2, for example, a ground speed as high as 8.6 m/sec was recorded, acceleration reached 0.1 m/sec^2, and the maximum altitude displacement in the 20-min test period was 54 m. The PIBAL wind speed was only 7.7 to 8.2 m/sec at float altitude, but the wind profiles shown with the horizontal trajectory,

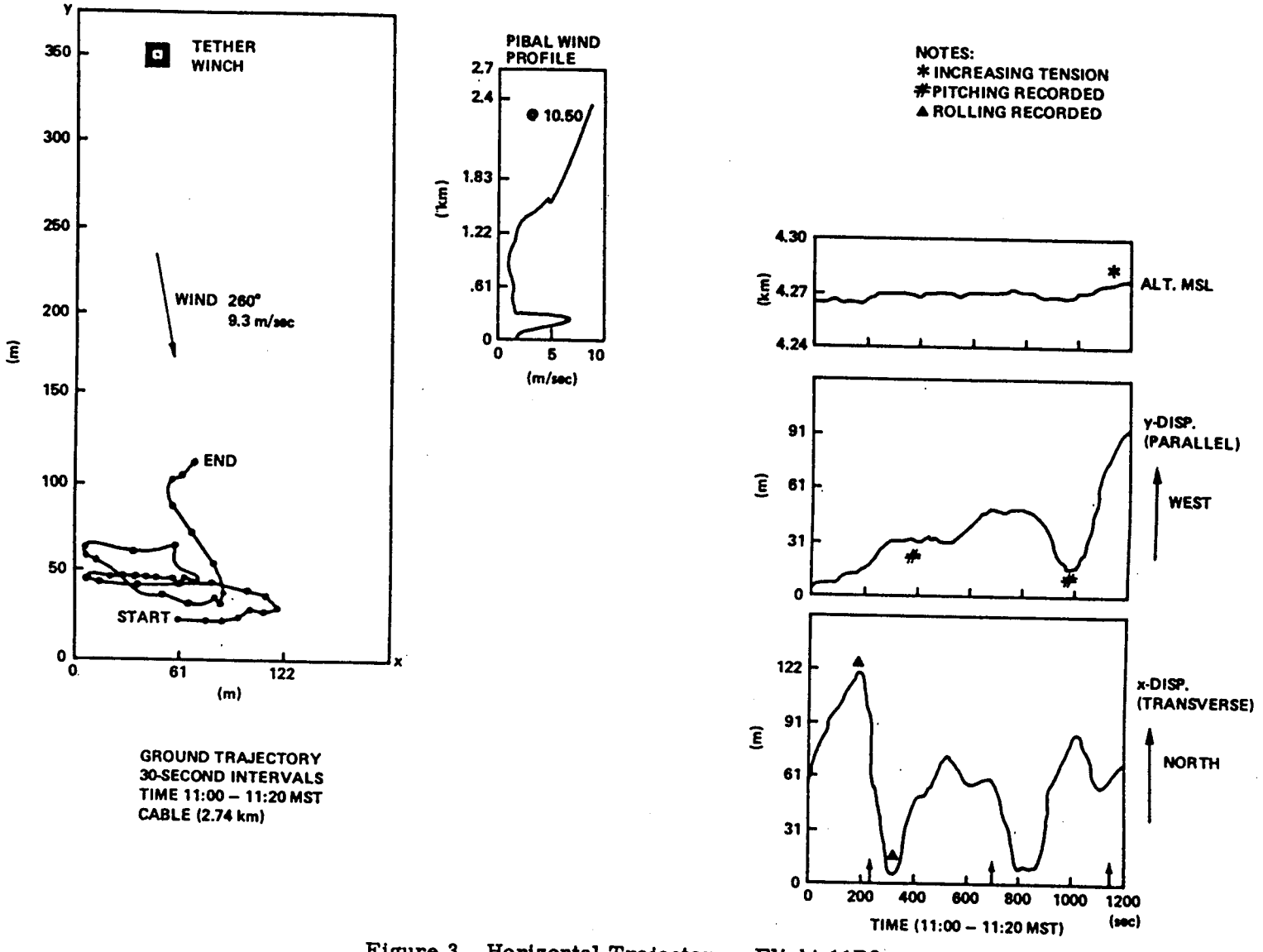

Figure 3. Horizontal Trajectory - Flight 11R3

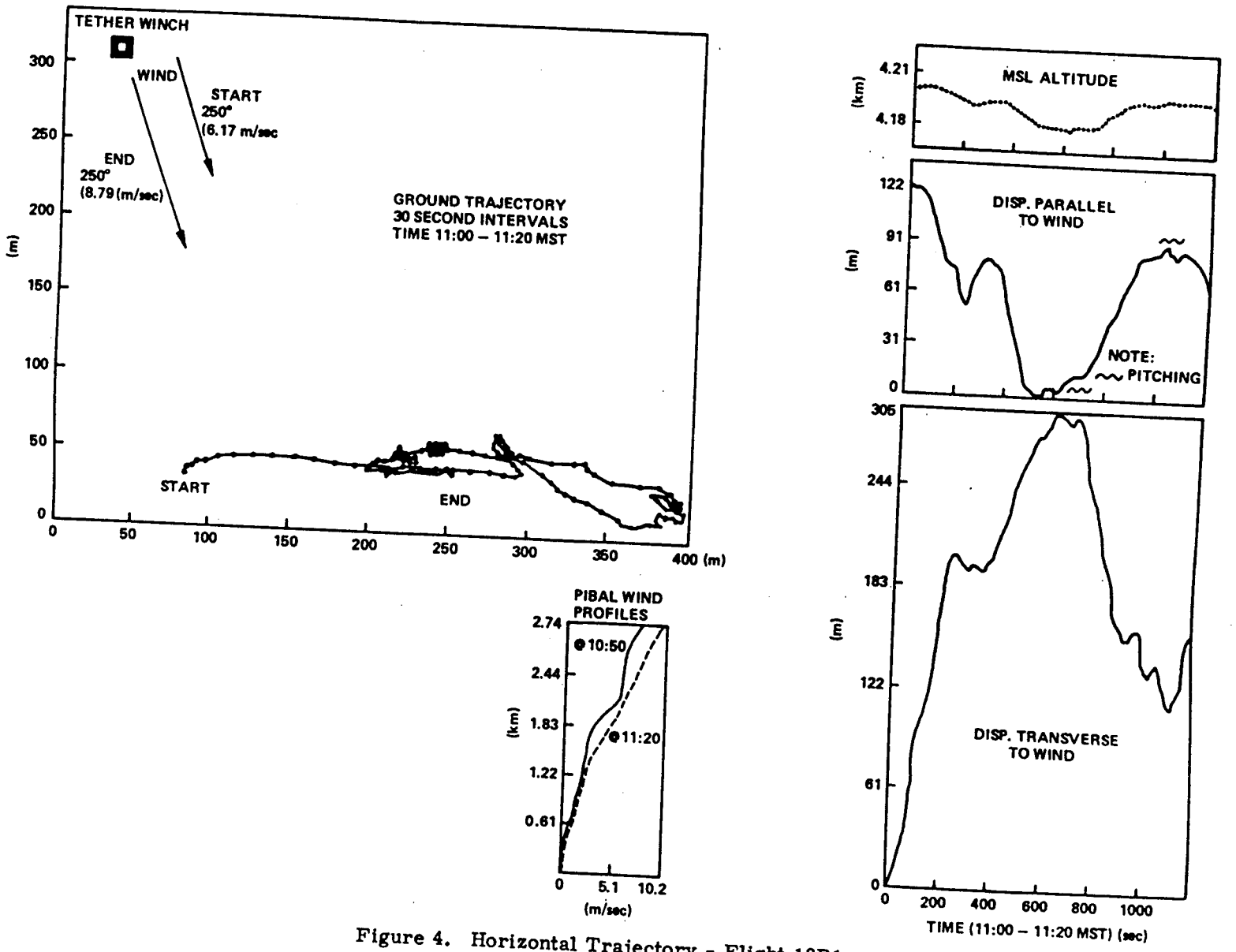

Figure 4. Horizontal Trajectory - Flight 12R1

Figure 5, show that there had been an increase in the winds along the length of the cable sometime during the test interval. (Unfortunately, due to a malfunction, anemometer data were not recorded during this flight.) For one 6.7-min period the balloon hovered above an area less than 91 m × 91 m.

Figure 6 shows the horizontal trajectory converted to displacements parallel and transverse to the wind direction at balloon height. The rolling and pitching motions can be directly associated with these directions. During the more rapid, large excursions that occurred between 750 and 1200 sec, the package was gradually rolling to reach the maximum roll displacement (16°) at the time of maximum transverse displacement. Brief episodes of pitching motion coincided with sharp reversals in the balloon's longitudinal motion; in one instance the angle of pitch reached 18.2°.

2.1.4 FLIGHT 13R2

The highest average wind speed during these tests, 14 m/sec, occurred during Flight 13R2. The cable length was 2.67 km. The horizontal trajectory, Figure 7, clearly shows the tendency of these balloons to produce ground tracks resembling figure eights. Maximum ground speed was 9.4 m/sec, and average anemometer wind speed was 14 m/sec, with one peak at 22 m/sec. Note the wind profile along the cable as detected by PIBAL just before this test. Not only were the winds near 609 m AGL unusually high compared with the other tests, there were also large gradients. When the test ended, this condition had changed, with winds generally 7.2 to 8.7 m/sec at all levels below the balloon. Predictably, the largest excursions occurred during the first half of the test.

2.2 Flights on the 1.52 km Cable

2.2.1 GROUND TRAJECTORIES

Tables 2(a) and 2(b) summarize the results of the tests using the 1.52 km cable. Figure 8 shows the horizontal trajectory for Flight 11R4, when the wind profile generally was below 2.6 m/sec; Figure 9, for 16R1, when winds along the cable were 6.2 m/sec or less, and the balloon-level wind was 5.1 to 6.7 m/sec; and Figure 10, for 16R5, when cable winds were 7.7 m/sec or higher, and balloon-level wind was 5.1 to 8.7 m/sec. Due to the increased drag forces from the steady components of the winds, the displacement of the balloon from the winch was greater in higher wind fields. Note, however, that the extent of wander was unrelated to the balloon-level average wind speed. There was greatest wander (Figure 8) when the average wind speed was least; and the area of wander at 8.7 m/sec balloon-level wind was not appreciably different from the wander at 5.1 to 6.7 m/sec (Figures 9 and 10). Closer examination shows that without the

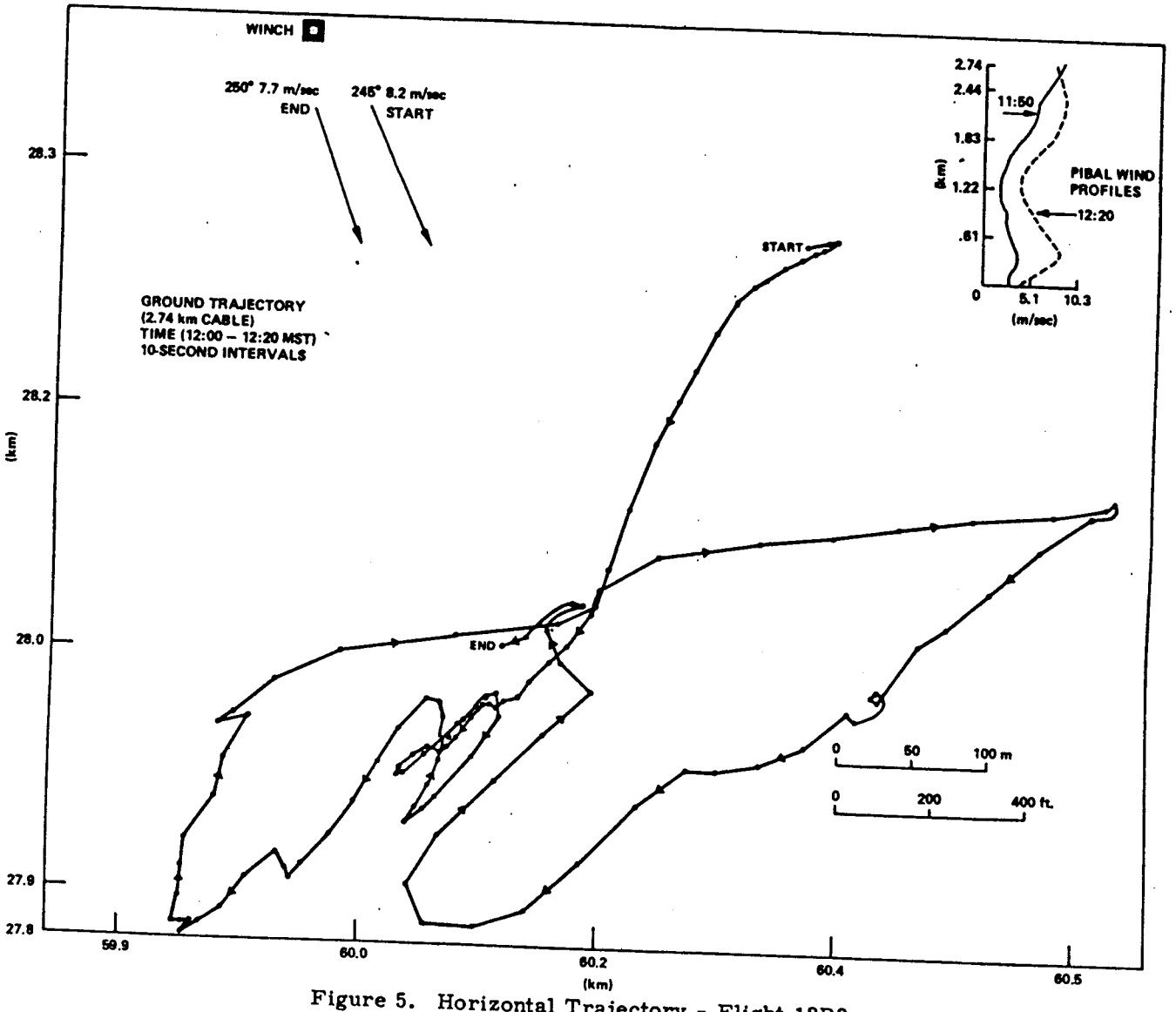

Figure 5. Horizontal Trajectory - Flight 12R2

two unusually large excursions shown by dotted line on Figure 8, and the one unusual excursion on Figure 9, the areas of wander are quite similar for all three tests. Obviously the outer bounds of the areas of wander are reactions to isolated gusts.

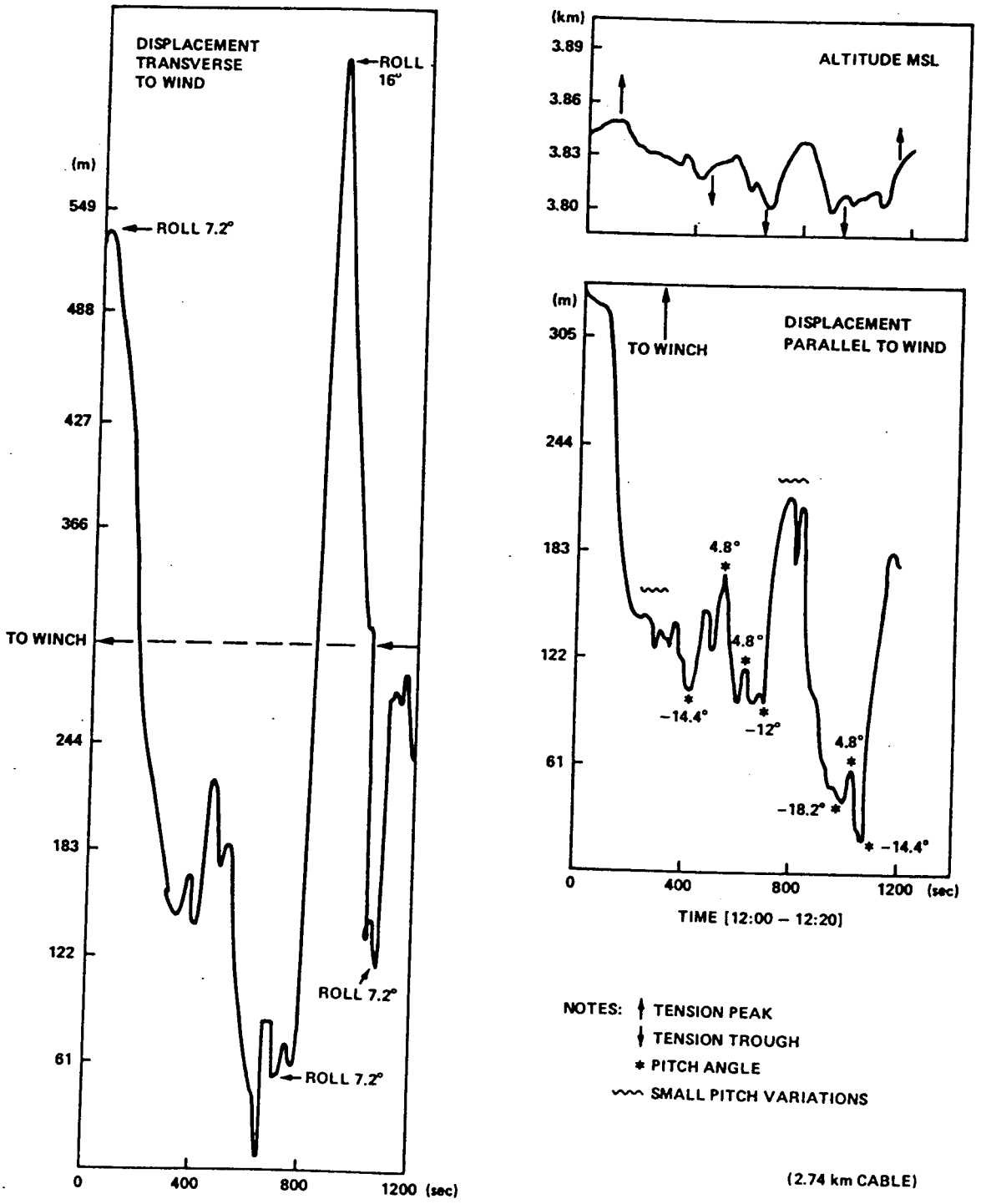

Figure 6. Horizontal Displacement Relative to the Wind vs Time, Flight 12R2

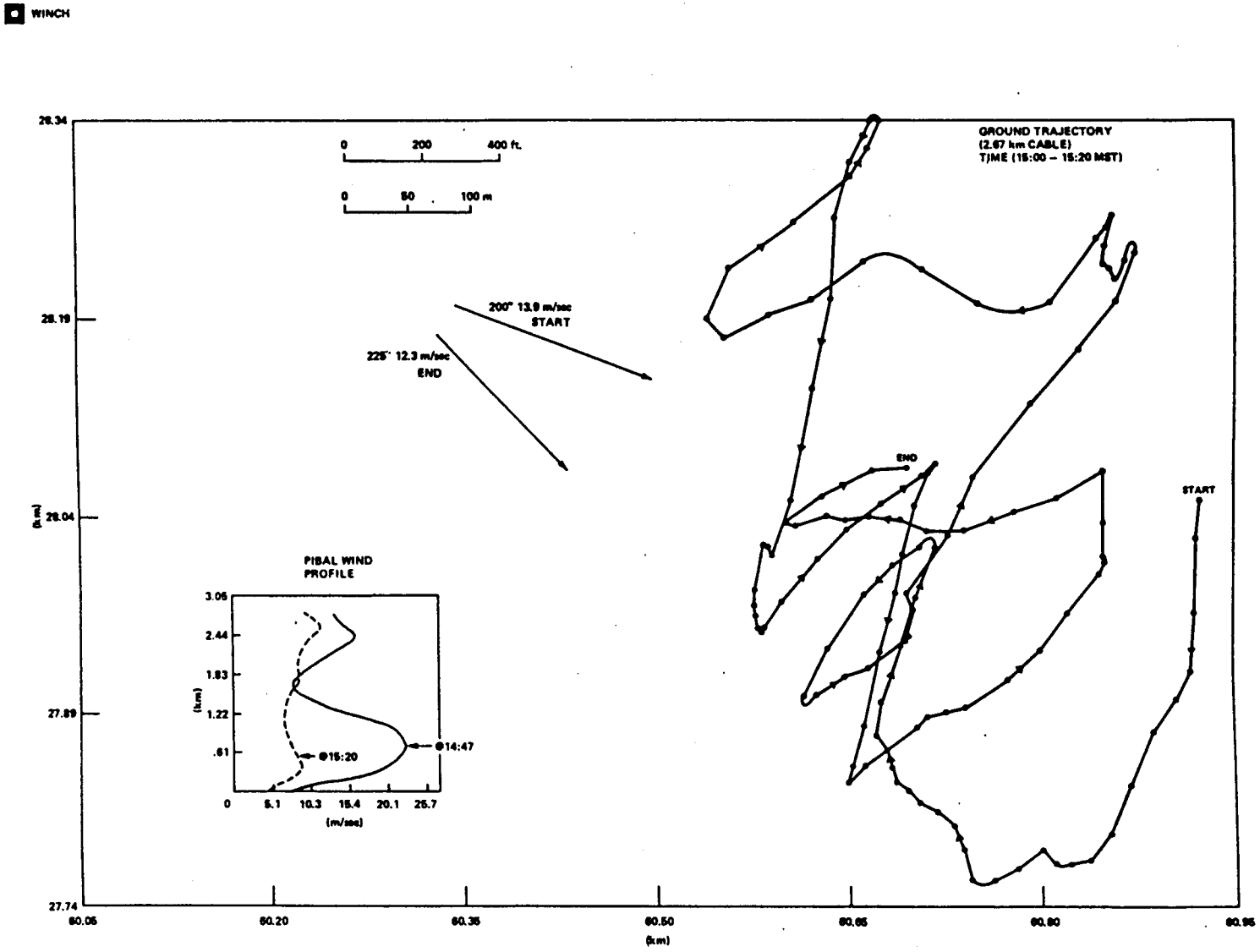

Figure 7. Horizontal Trajectory - Flight 13R2

Table 2(a). (English Units)
Flight Data Using 5000-Ft Cable

Flight No. / Start Time MST	PIBAL Wind at Balloon Alt.		Equil. Distance	Range in Alt. (ft) During 20 Min	Avg. Alt. AGL	Max. Wander	Max. Tang. Acceleration	Cable Tension (lb)	
	Speed (kt)	Dir. (deg)	d (ft)		(ft)	(ft)		Min. / Max.	Typical
11R4 / 12:00	<10	220	150	72	5229	1120	0.1 G	1550 / 3700	2600
12R3 / 13:00	13 8	230 250	600 360	138	5035	1100 800	0.1 G	1100 / 4500	2900
12R4 / 1400	10 12	240 235	570	94	5047	1210	0.1 G	1900 / 4500	2600
16R1 / 1100	13 10	190 190	630	94	4992	850 760	0.1 G	2400 / 2950	2600
16R2 / 12:00	17	200	640	159	4994	920	0.1 G	1850 / 4100	2600
16R4 / 1400	14 16	200 228	930 1360	120	4916	830 920	0.1 G	1800 / 3850	2800
16R5 / 1500	17 10	205 200	1400 1050	169	4818	710 840	0.1 G	1650 / 3600	2650

Table 2(a). (Metric Units)
Flight Data Using 1.52 km Cable

Flight No. / Start Time MST	PIBAL Wind at Balloon Alt.		Equil. Distance	Range in Alt. (m) During 20 Min	Avg. Alt. AGL	Max. Wander	Max. Tang. Acceleration	Cable Tension (N)	
	Speed m/sec	Dir. (deg)	d (m)		(m)	(m)	m/sec^2	Min. / Max.	Typical
11R4 / 12:00	5.1	220	46	22.0	1594	341	1.0	69.1×10^2 / 165×10^2	116×10^2
12R4 / 14:00	5.1 6.2	240 235	174	28.7	1538	369	1.0	84.6×10^2 / 200×10^2	116×10^2
12R3 / 13:00	6.7 4.1	230 250	183 110	42.1	1535	335 244	1.0	49.0×10^2 / 200×10^2	129×10^2
16R1 / 11:00	6.7 5.1	190 190	192	28.7	1522	259 232	1.0	107×10^2 / 131×10^2	116×10^2
16R2 / 12:00	8.7	200	195	48.5	1522	280	1.0	82.4×10^2 / 183×10^2	116×10^2
16R4 / 14:00	7.2 8.2	200 228	284 415	36.6	1498	253 280	1.0	81.2×10^2 / 172×10^2	125×10^2
16R5 / 15:00	8.7 5.1	205 200	427 320	51.5	1469	216 256	1.0	73.5×10^2 / 160×10^2	118×10^2

Table 2(b). (English Units)
Flight Data Using 5000-Ft Cable (Cont)

Flight No.	Maximum Ground Speed During a Typical Excursion (ft/sec)	Maximum Ground Speed During the Test (ft/sec)	Anemometer Wind (kt) Range	Anemometer Wind (kt) Average	Maximum Pitch Angle (degrees)	Maximum Roll Angle (degrees)
11R4	16	26	<8-24	10	16.8	14.4
12R3	15	19	No Data		12	7.2
12R4	12	25	18-27	18	14.4	7.2
16R1	10	21	<10-27	40 ?	9.6	3.6
16R2	13	26	<10	16	16.8	7.2
16R4	15	18	10-38	15	14.4	7.2
16R5	10	21	<8-38	18	12	7.2

Table 2(b). (Metric Units)
Flight Data Using 1.52 km Cable (Cont)

Flight No.	Maximum Ground Speed During a Typical Excursion (m/sec)	Maximum Ground Speed During the Test (m/sec)	Anemometer Wind (m/sec) Range	Anemometer Wind (m/sec) Average	Maximum Pitch Angle (degrees)	Maximum Roll Angle (degrees)
11R4	4.9	7.9	<4.1 - 12.3	5.1	16.8	14.4
12R3	4.6	5.8	No Data		12	7.2
12R4	3.7	7.6	9.3 - 13.9	9.3	14.4	7.2
16R1	3.0	6.4	<5.1 - 13.9	20.6	9.6	3.6
16R2	4.0	7.9	<5.1	8.2	16.8	7.2
16R4	4.6	5.5	5.1 - 19.5	7.7	14.4	7.2
16R5	3.0	6.4	4.1 - 19.5	9.3	12	7.2

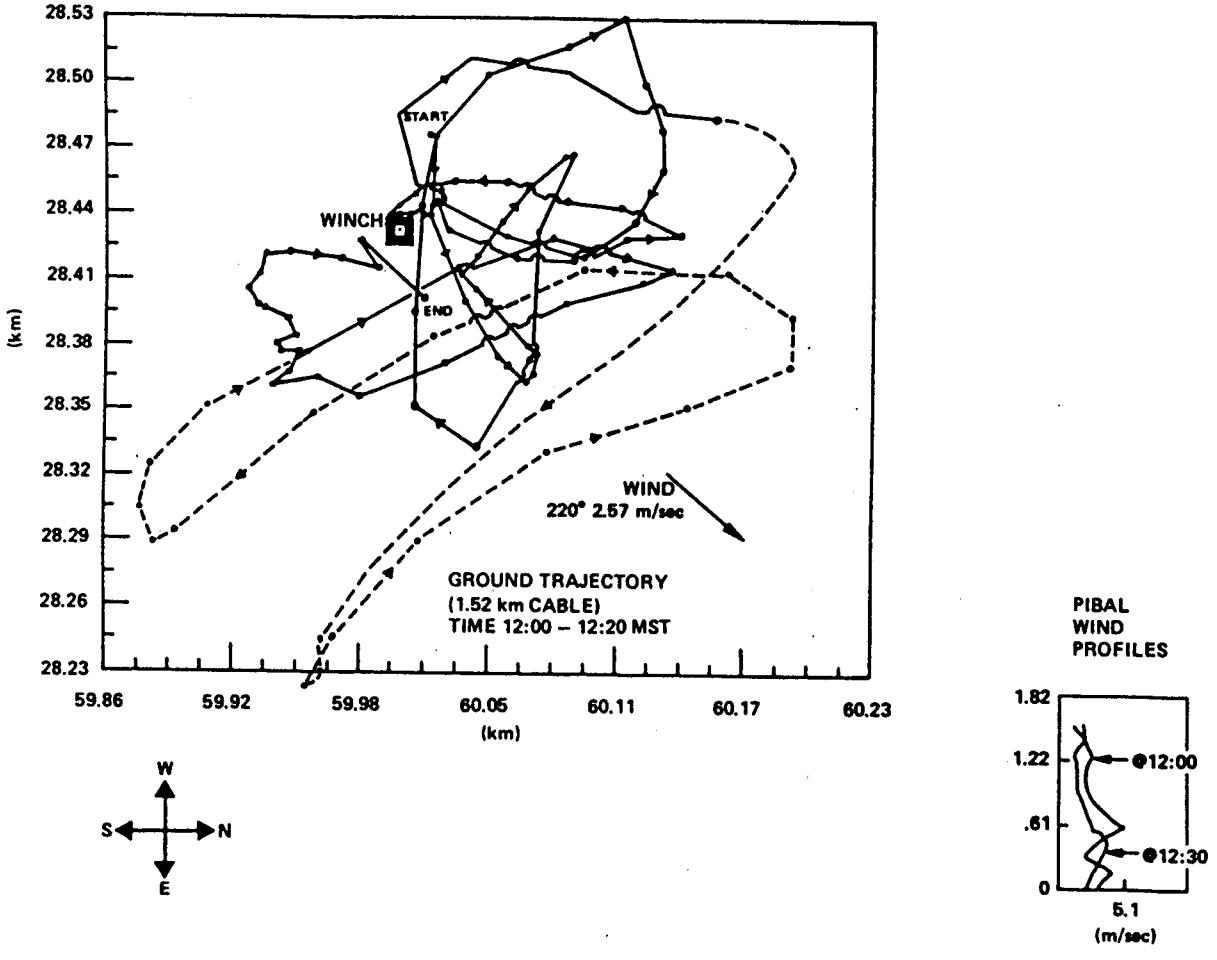

Figure 8. Horizontal Trajectory - Flight 11R4

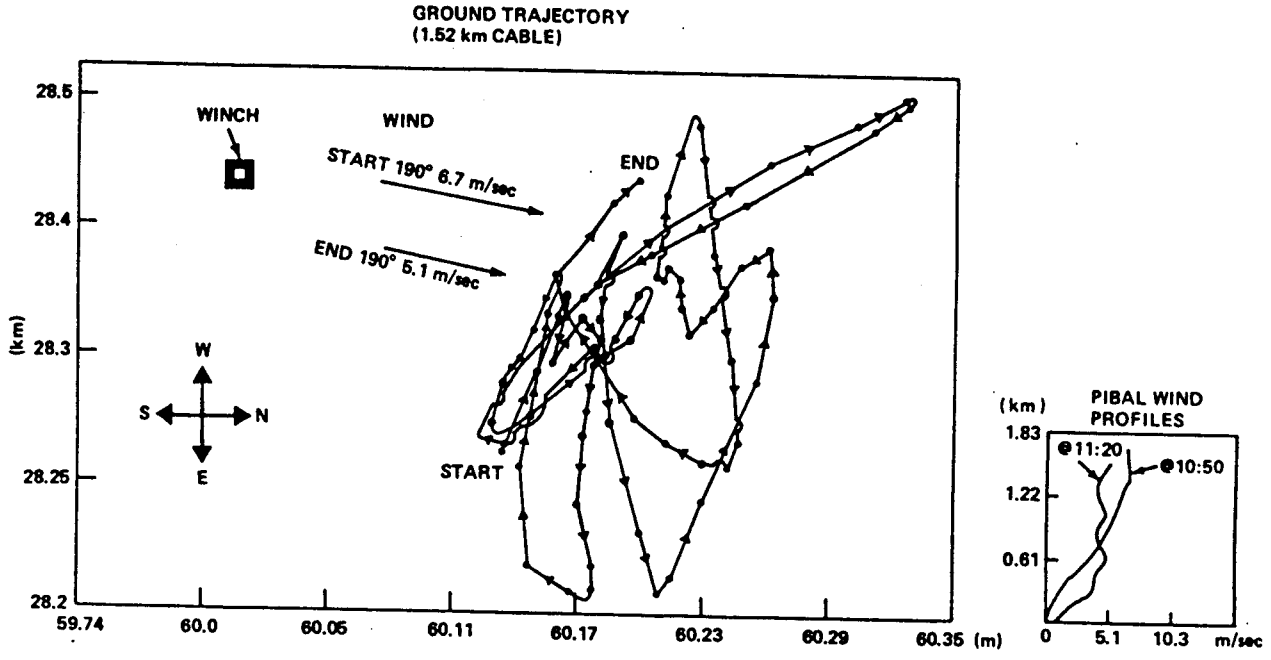

Figure 9. Horizontal Trajectory - Flight 16R1

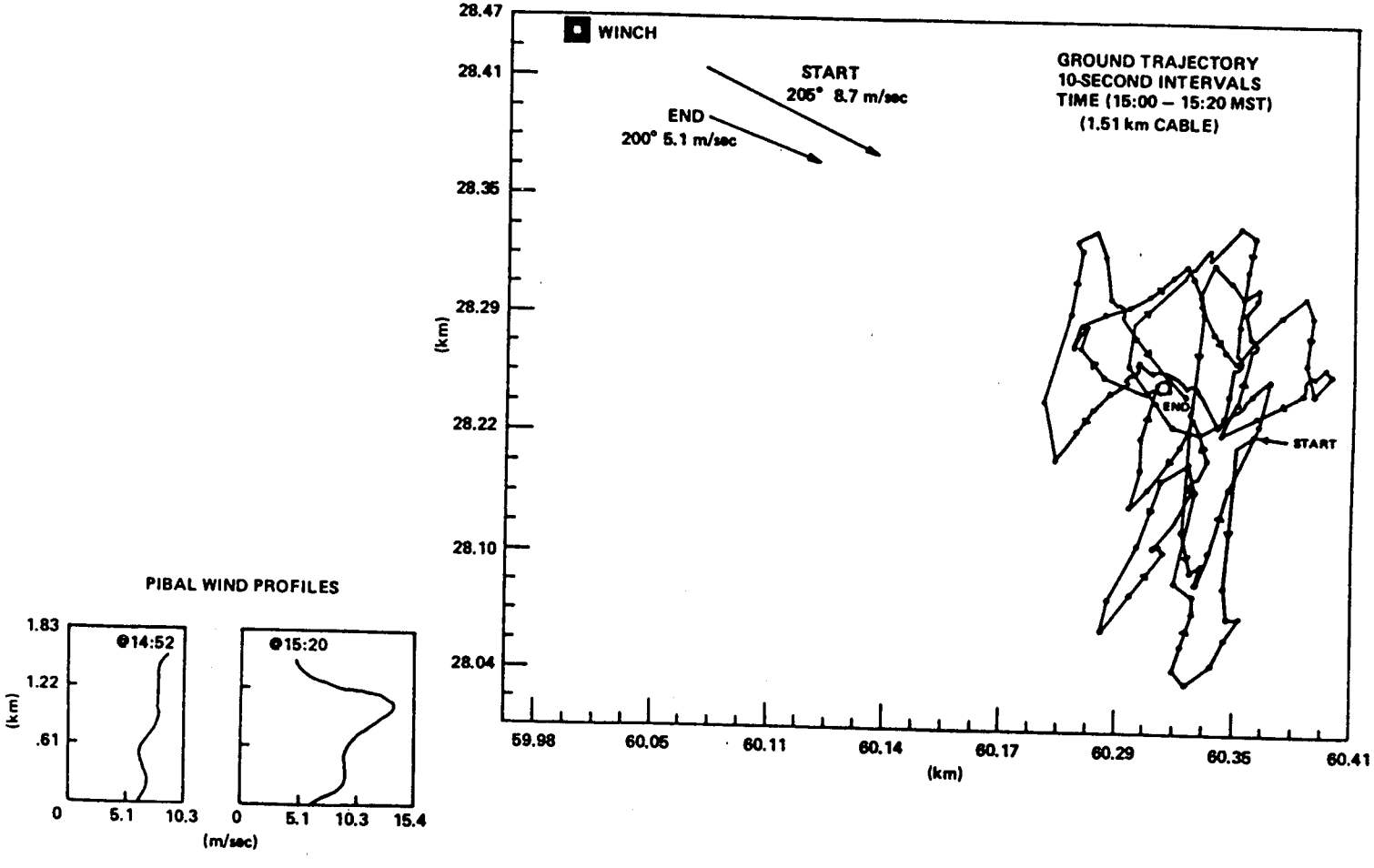

Figure 10. Horizontal Trajectory - Flight 16R5

Figures 11 through 14 are ground trajectories for the remaining flights using the 1.52 km cable. The patterns of wander in Figures 11, 12, and 13 are quite similar, although the corresponding PIBAL wind profiles are different. From Figure 14, there is no doubt that flight conditions must have changed abruptly soon after the start of the test. This flight underscores the principal uncertainty in interpreting tethered-balloon flight motion data—usually we have no independent means of monitoring the instantaneous wind.

2.2.2 FLIGHT 16R2

Flight 16R2 is considered typical of the flight performance on the 1.52 km cable. Displacements transverse and parallel to the PIBAL wind are plotted in Figure 15. Figure 16 shows the tangential acceleration and speed relative to ground, tension at the confluence point, slant range of target from winch, and altitude versus time.

The closest correlation among the data is between tension and slant range (Figure 16). When tension was the greatest, the balloon was near to the winch in terms of horizontal displacement parallel to the wind direction (see Figures 15 and 16) and flying high; momentarily the balloon had maximum dynamic lift and the increased tension stretched the cable. Conversely, when tension was least, the slant range and altitude also were at, or almost at, minimum, and the balloon was at maximum horizontal displacement in the wind direction and at a point of inflection in its motion transverse to the wind (see points T_{min}). At times of peaks in cable tension, the tangential acceleration along the balloon trajectory was not maximum [Figure 16] (but the radius of curvature was small and the centripetal acceleration correspondingly was high). At the times when acceleration along the trajectory was maximum, there were secondary peaks of tension.

When the package rolled (occasionally up to 14.4°) the rolling motion was in phase with the large transverse displacements.

2.3 Flight on 914 m Cable

Flight 11R2 (Table 3) was very steady in 2.1 m/sec winds. Altitude range was 1.8 m, and the area of wander, 14.6 × 40.8 m. Balloon displacement was about 47.2 m from the winch. Roll angle never exceeded 3.6°, and pitch varied ±1.2° to about 4.8°. Maximum ground speed was 0.91 m/sec, and speed relative to the wind (or vice versa) averaged 5.1 m/sec.

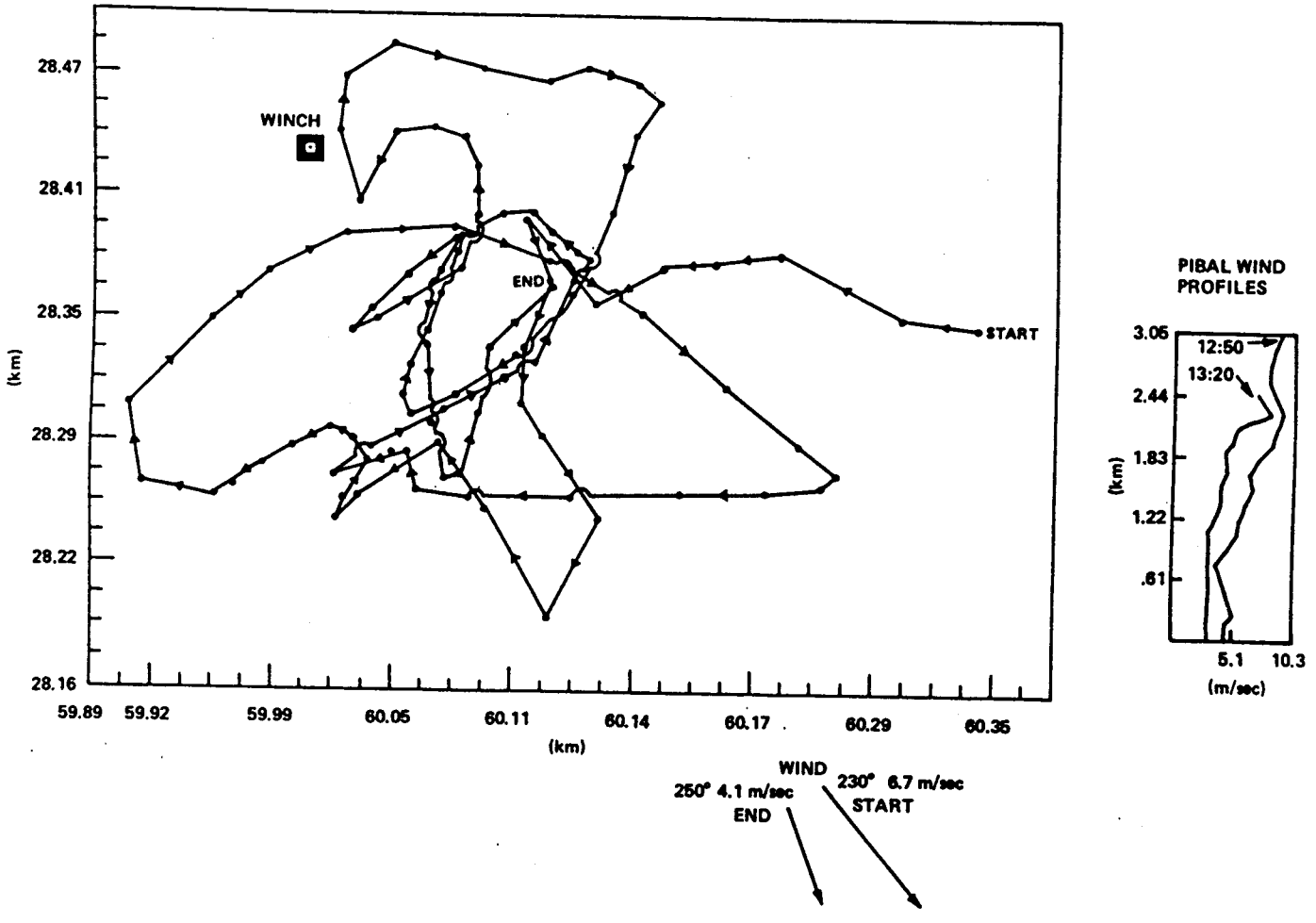

Figure 11. Horizontal Trajectory - Flight 12R3

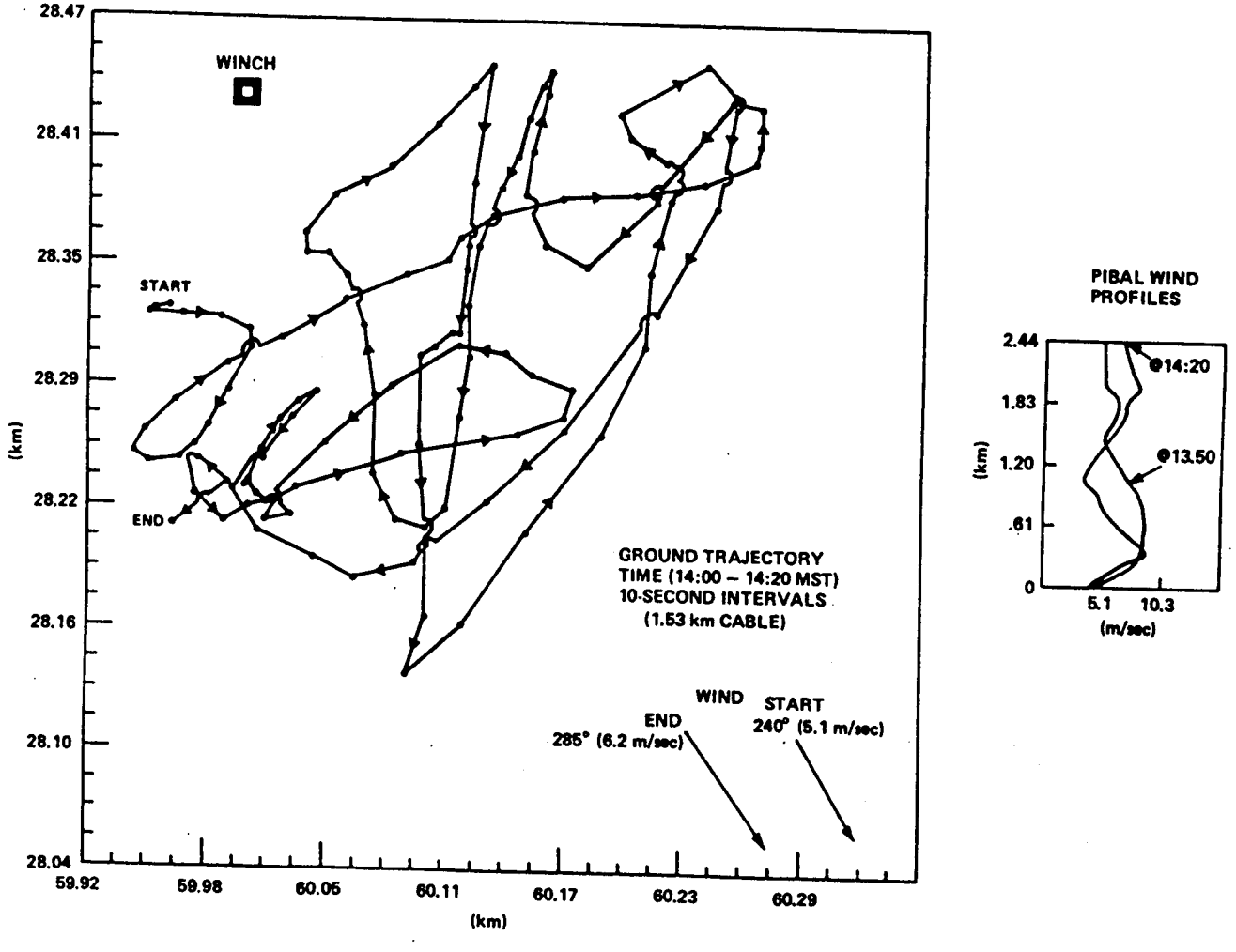

Figure 12. Horizontal Trajectory - Flight 12R4

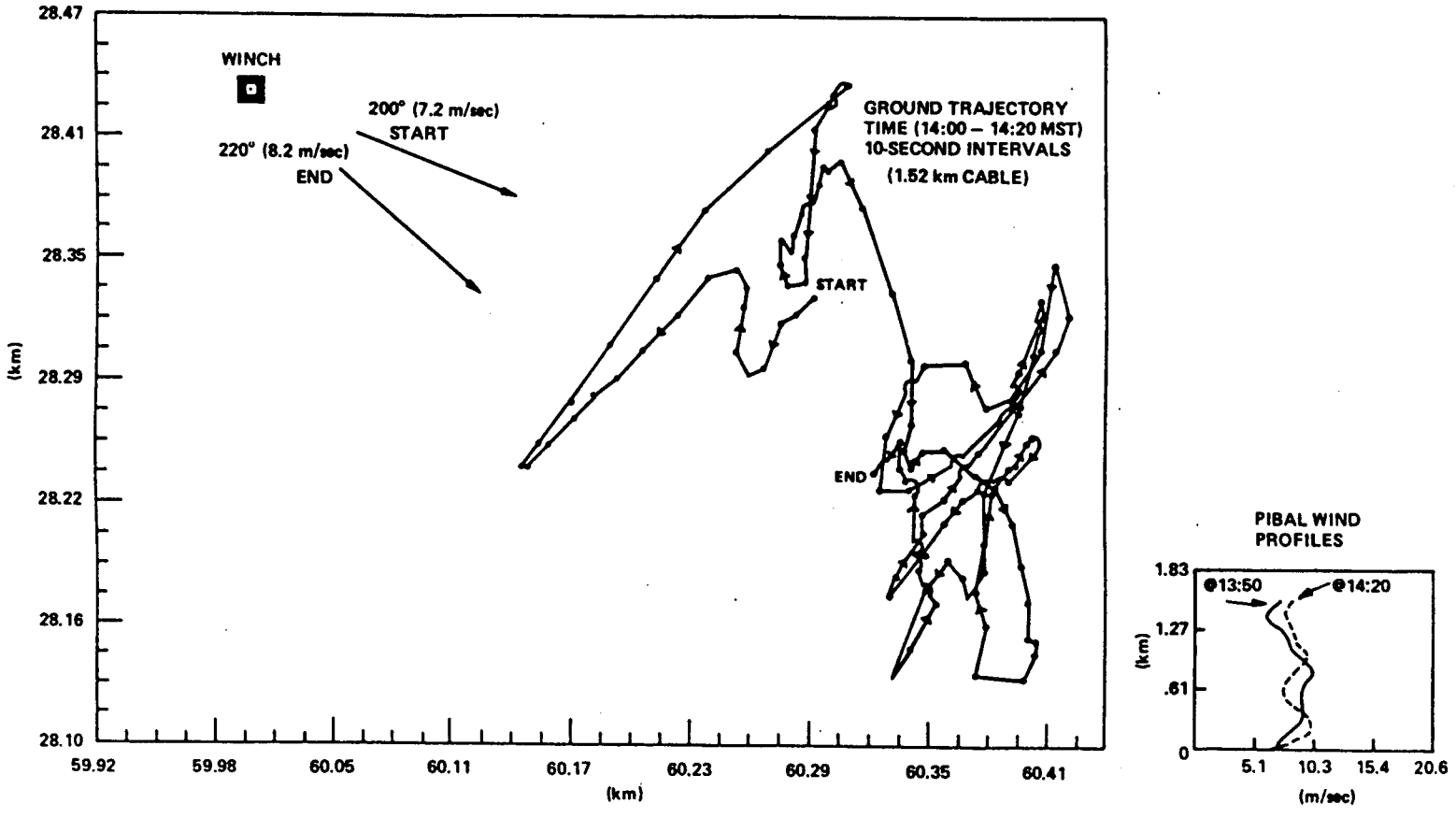

Figure 13. Horizontal Trajectory - Flight 16R4

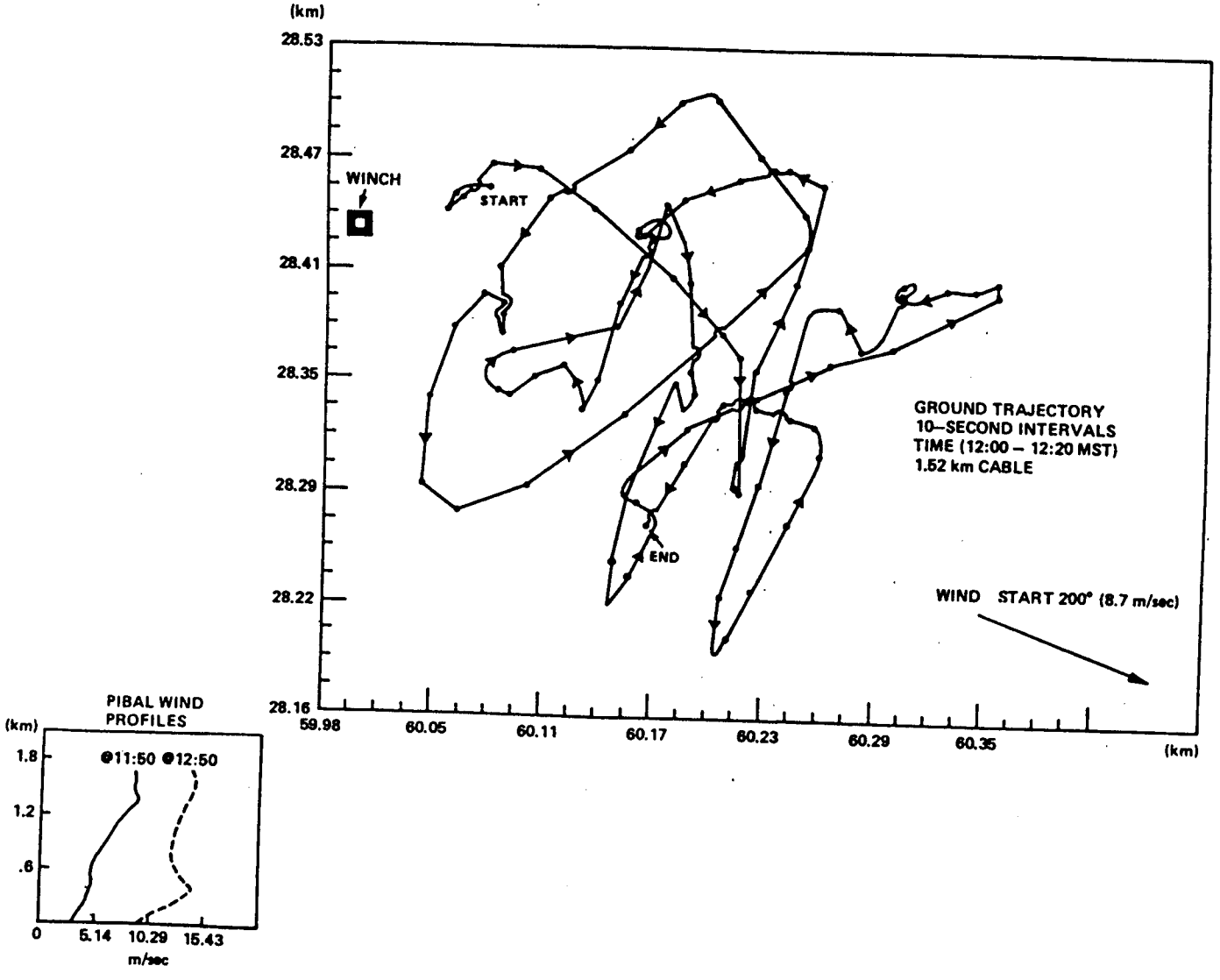

Figure 14. Horizontal Trajectory - Flight 16R2

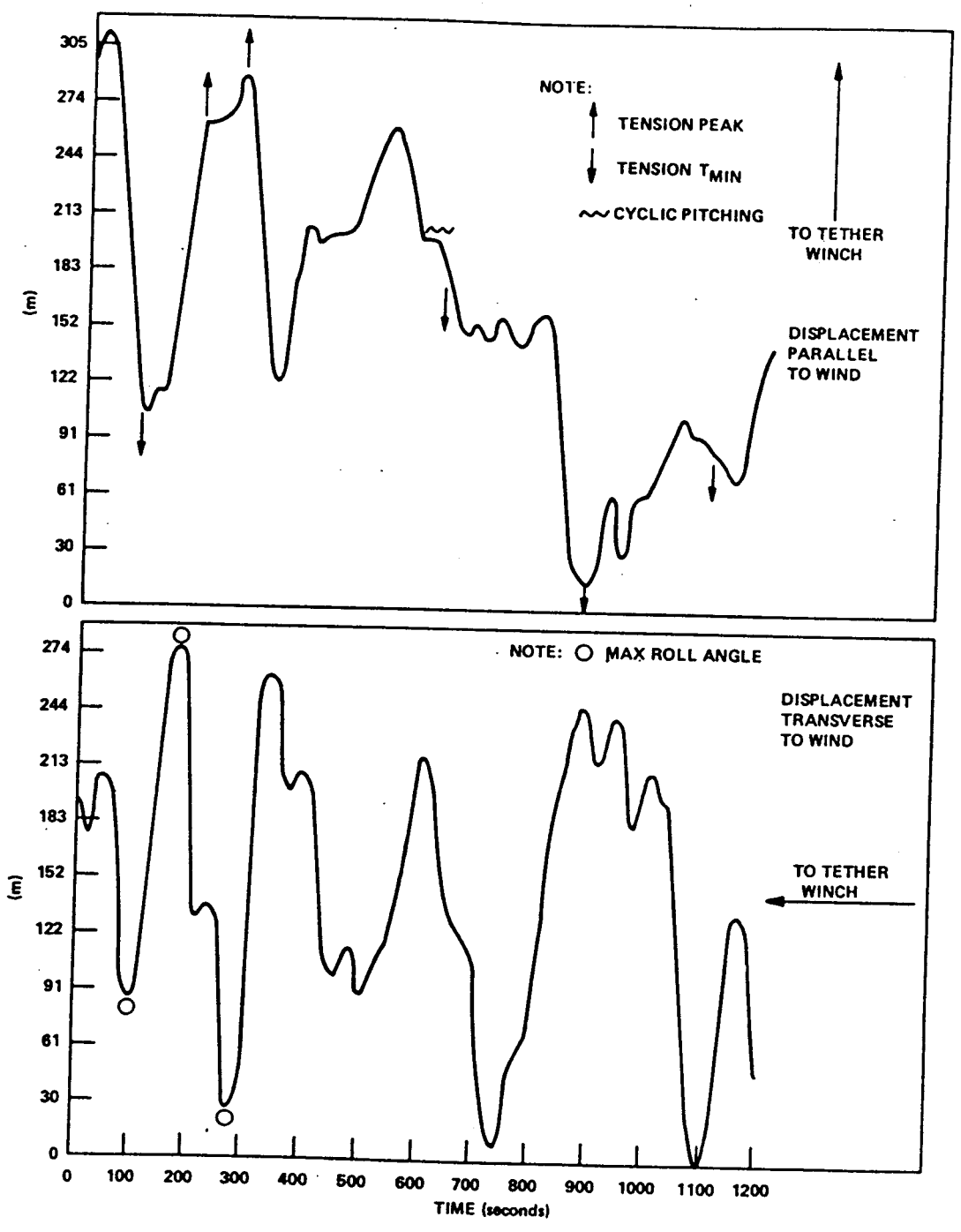

Figure 15. Flight Data - Flight 16R2

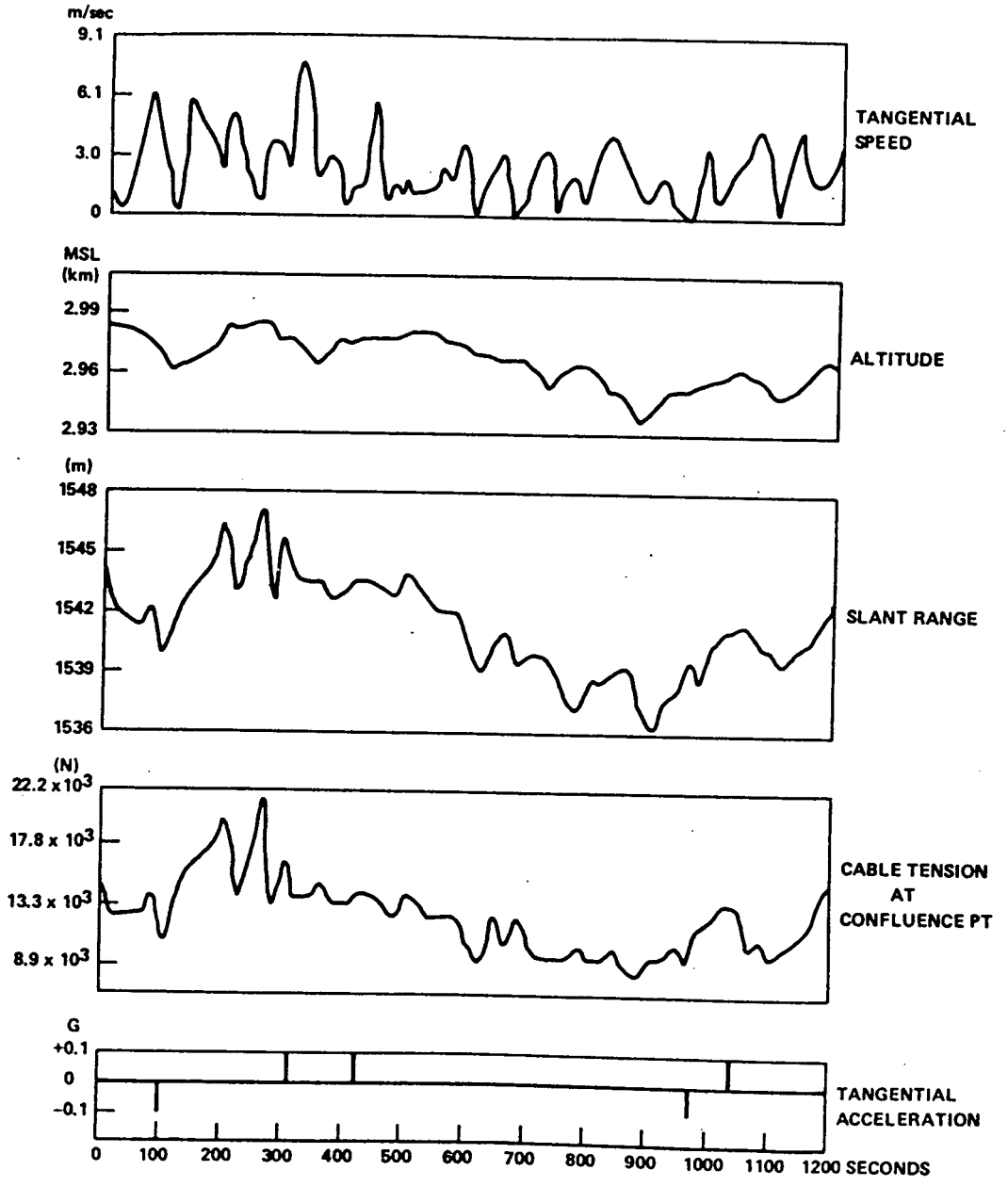

Figure 16. Flight Data - Flight 16R2 (Cont)

Table 3(a). (English Units)
Flights on Various Lengths of Cable

Cable Length (ft)	Flight No. / Start Time MST	PIBAL Wind at Balloon Alt.		Equil. Distance d (ft)	Range in Alt. (ft) During 20 Min	Avg. Alt. AGL (ft)	Max. Wander (ft)	Max. Tang. Acceleration	Cable Tension (lb)	
		Speed (ft)	Dir. (deg)						Min. / Max.	Typical
3000	11R2 / 09:00	4	345	155	6	3134	142	<0.1 G	2500 / 2800	2650
1000	11R1 / 08.00	3.5	310	20	4	1049	47	<0.1 G	2600	2600
1000	12R5	8 9	230 250	110	52	1054	450	0.1 G	1750 / 3550	2200
6000	17R2	11	240	1200	196	6023		0.1 G	No Telemetry	

Table 3(a). (Metric Units)
Flights on Various Lengths of Cable

Cable Length (m)	Flight No. / Start Time MST	PIBAL Wind at Balloon Alt. Speed (m/sec)	PIBAL Wind at Balloon Alt. Dir. (deg)	Equil. Distance d (m)	Range in Alt. (m) During 20 Min	Avg. Alt. AGL (m)	Max. Wander (m)	Max. Tang. Acceleration (m/sec^2)	Cable Tension (N) Min. / Max.	Cable Tension (N) Typical
914	11R2 / 09:00	2.1	345	47.2	1.8	955.2	43	<1	111×10^2 / 125×10^2	118×10^2
305	11R1 / 08:00	1.8	310	6.1	1.2	319.7	14	<1	116×10^2 / 116×10^2	116×10^2
305	12R5	4.1 4.6	230 250	33.5	15.8	321.3	137	1	78.0×10^2 / 158×10^2	98.0×10^2
1829	17R2	5.7	240	366	59.7	1835.8	-	1	No Telemetry	

Table 3(b). (English Units)
Flights on Various Lengths of Cable (Cont)

Flight No.	Maximum Ground Speed During a Typical Excursion (ft/sec)	Maximum Ground Speed During the Test (ft/sec)	Anemometer Wind (ft) Range	Anemometer Wind (ft) Average	Maximum Pitch Angle (degrees)	Maximum Roll Angle (degrees)	Cable Length (ft)
11R2	1	3	8 - 15	10	<2.4	<3.6	3000
11R1	<1	2	<10		4.8	<1.8	1000
12R5	10	19	<8 - 27	18	16.8	14.4	1000
17R2	12	29	No Telemetry				

Table 3(b). (Metric Units)
Flights on Various Lengths of Cable (Cont)

Flight No.	Maximum Ground Speed During a Typical Excursion (m/sec)	Maximum Ground Speed During the Test (m/sec)	Anemometer Wind (m/sec) Range	Anemometer Wind (m/sec) Average	Maximum Pitch Angle (degrees)	Maximum Roll Angle (degrees)	Cable Length (m)
11R2	0.3	0.91	4.1 - 7.7	5.1	2.4	3.6	914
11R1	<0.3	0.61	<5.1	-	4.8	1.8	305
12R5	3.0	5.8	<4.1 - 13.9	9.3	16.8	14.4	305
17R2	3.7	8.8	No Telemetry				1829

2.4 Flights on 304.8 m Cable

2.4.1 FLIGHT 11R1

Flight 11R1 (Table 3) was in very calm wind. The balloon floated directly above the winch and the package remained within an area of only 12.5 × 7.3 m. Maximum range in altitude was 1.2 m and maximum ground speed 0.61 m/sec. Balloon displacement was about 6.1 m from the winch. Cable tension was very steady, there was no measurable roll, and pitch occasionally reached a maximum of 2.4 degrees.

2.4.2 FLIGHT 12R5

On Flight 12R5 the PIBAL wind was 4.1 to 4.6 m/sec, but the values of ground speed (5.8 m/sec), and average wind speed indicated by the anemometer (5.5 m/sec), suggest that the PIBAL wind speed value is too low.

At this low altitude, due to higher air density, the drag force is larger than at higher altitudes at the same wind speeds and the impulses due to similar gusts (that is, the same change in speed vs time) are also stronger. The area of wander was 131 m × 113 m; maximum range in altitude was 15.8 m. The cable tension record shows strong damped oscillations at approximately 0.2 Hz – with the short tether length the cable was vibrating, and the package was pitching (Figure 17).

2.5 Ambient Wind Speed (PIBAL vs Anemometer Measurement)

Values for ambient wind speed were determined using both PIBALS and a balloon-borne cup anemometer. Each of these devices has different inherent errors, but both methods are commonly used to obtain a measure of the steady state parameter we call ambient wind speed aloft. From an operational standpoint, then, a comparison of the data is useful.

The standard PIBAL is inflated with a measured free lift and thereby assumed to have a known, constant vertical ascent rate;[1] on this basis the altitude at successive intervals after PIBAL release is determined. At 1-min intervals, azimuth and elevation angles of the balloon position are read from the tracking theodolite. The direction and speed of the PIBAL are computed from these data and averaged over a suitable interval of height (152 m for these tests). The PIBAL speed vector is taken as the wind speed vector. In addition to the uncertainty due to taking a single sample in a dynamic atmosphere, the assumption of a constant vertical ascent rate can introduce a large error in a PIBAL-determined wind speed.

---

1. Manual of Winds Aloft Observations, Circular O, Hq AWS, (MATS) USAF.

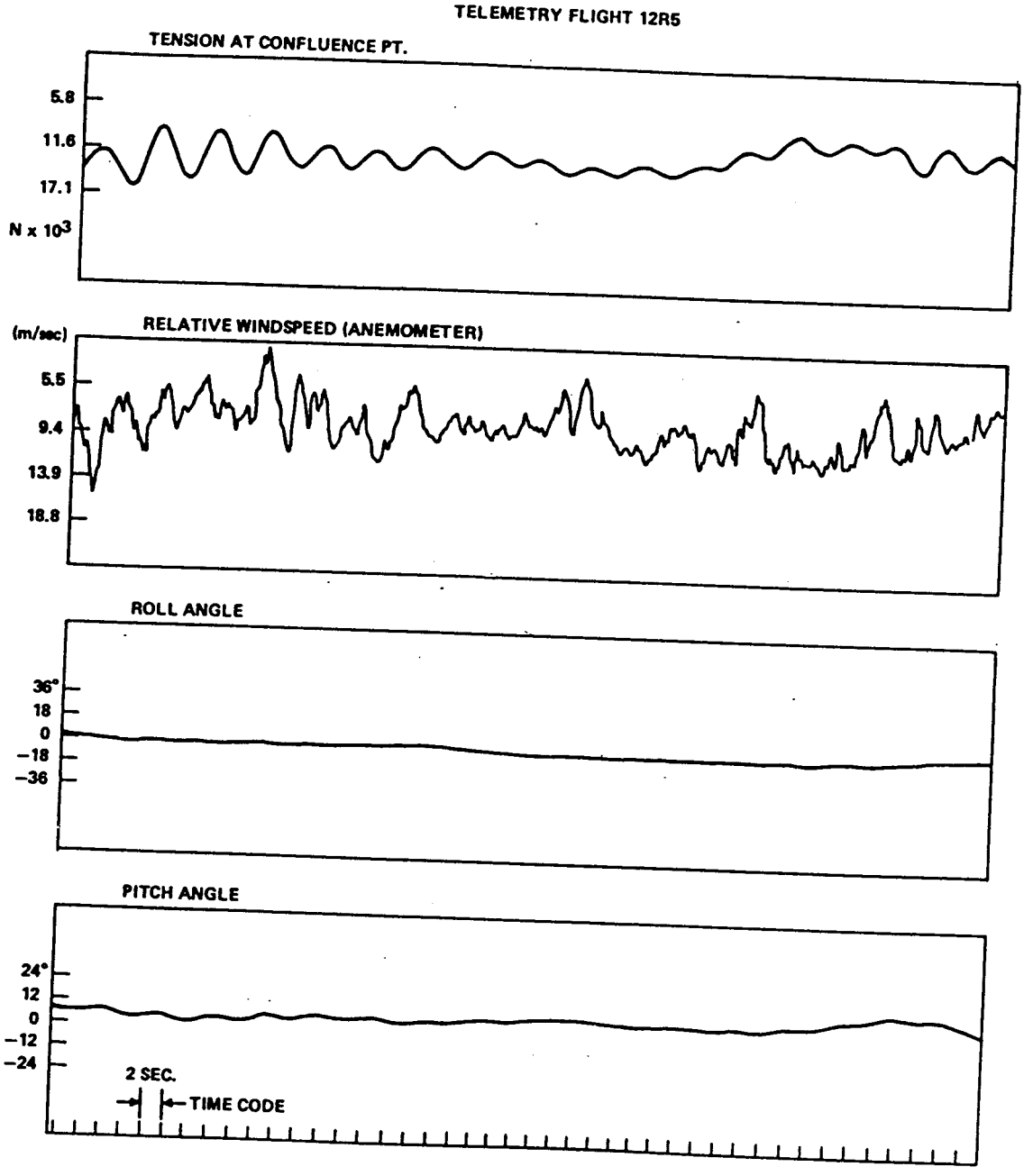

Figure 17. Telemetry Record: Tension and Pitch Angle vs Time

A balloon-borne anemometer always measures a wind speed relative to the motion of the balloon, rather than relative to ground. It affords frequent, or continuous sampling, however, and if the balloon is stable, if the anemometer is placed outside the boundary layer of the balloon, and if the relative wind speed remains above the anemometer threshold, then the average reading should be significant.

Figure 18 shows the average anemometer value obtained by graphically scaling the telemetry record for each 20-min test, plotted with the PIBAL data. (On two flights the winds were below threshold for the anemometer, and on one, data were not recorded.) For 11 flights the agreement is very good. Large deviations occurred for one flight each using 2.74, 1.52, 0.914, and 0.305-km cable length. Barring gross human errors in the observations, presumably the PIBAL sample was not typical of the ambient wind during those flights.

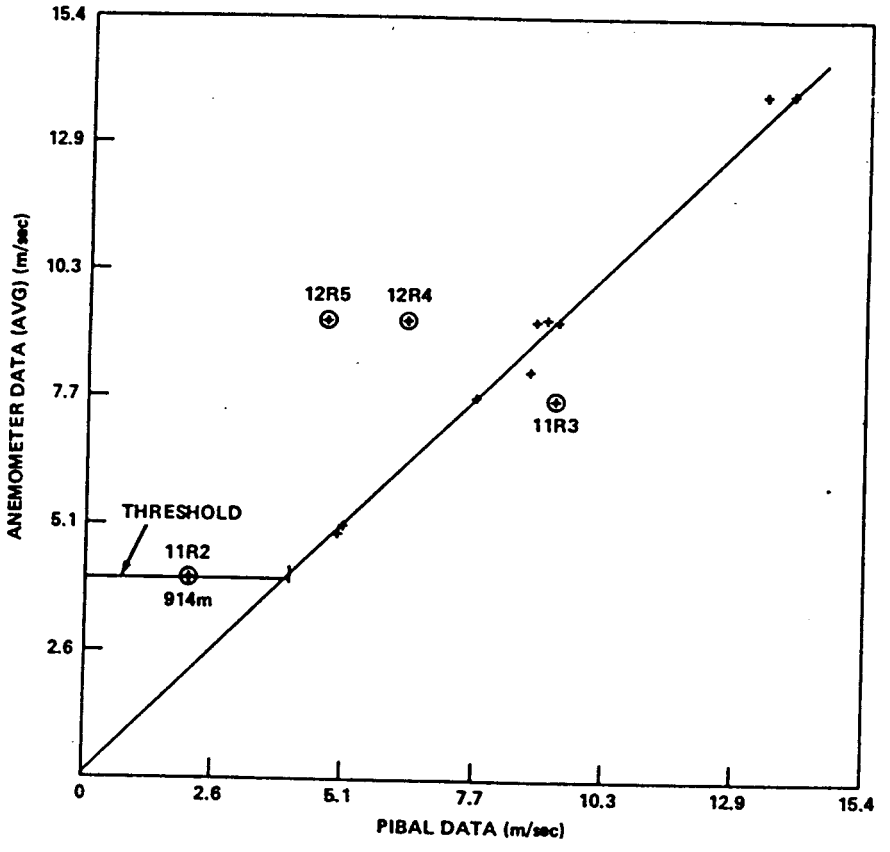

Figure 18. Average Anemometer Wind Speed vs PIBAL Wind Speed

2.6 Balloon Horizontal Displacement, d

For each flight test, an apparent balloon equilibrium position was established by examining the trajectory of the balloon in the horizontal plane and estimating the location on the graph above which the balloon tended to hover or about which it tended to wander. The distance between this location and the winch is arbitrarily defined as the horizontal displacement, d. (In view of the natural variability of the winds and the occurrence during some flights of a few unusually strong gusts, this graphical procedure was considered more appropriate than computational methods for d.)

2.6.1 DISPLACEMENT, d, VS AMBIENT WIND SPEED

Figure 19 shows values of d plotted versus the PIBAL-detected wind speed at balloon altitude, V_w, for nominal cable lengths, L, of 1.52 km and 2.74 km. These curves suggest a simple relationship between displacement and ambient wind speed for given lengths of the same cable. Figure 20 shows values of the logarithm of (d) to be roughly proportional to the logarithm of (V_w) for constant L. The relationship can be fairly well represented by the expression:

$$d = f(L)\, V_w^{1.7} \qquad (1)$$

in which the value of f (L) is determined by the intercept on the graph, Figure 20.

Thus, the data are in reasonable agreement with the basic theory: in equilibrium, the balloon displacement is determined by the lift and drag forces on the balloon, which are proportional to the second power of the relative wind speed – and also upon the air density at float altitude as well as the aerodynamic and gravitational forces along the cable, all of which are implicit in f (L).

The actual equations of equilibrium for a single-tethered balloon system in a steady wind are, in fact, far from being so simple, because the aerodynamic coefficients and the angle of attack of the aerodynamic-shape balloon vary with wind speed, and because the cable is immersed in a wind field in which the direction and speed of the wind can vary greatly along the length of the cable.* There are few, if any, useful tethered systems for which the cable aerodynamic forces are negligible; these forces can be the critical elements in the system performance.

* There are a number of recent analytical studies in which a computerized model of the cable is used to predict the cable profile and displacement of a tethered balloon system. The usual procedure is to write a program in which the cable shape is approximated by an arbitrary number of linked, linear segments. The effective air density and wind vector acting upon each segment are used to determine the aerodynamic forces on that segment. Starting at the confluence point, the equation of equilibrium is expressed for each consecutive segment in order to determine its displacement, orientation and tension, ending with those values at the lower extremity of the cable at the winch.

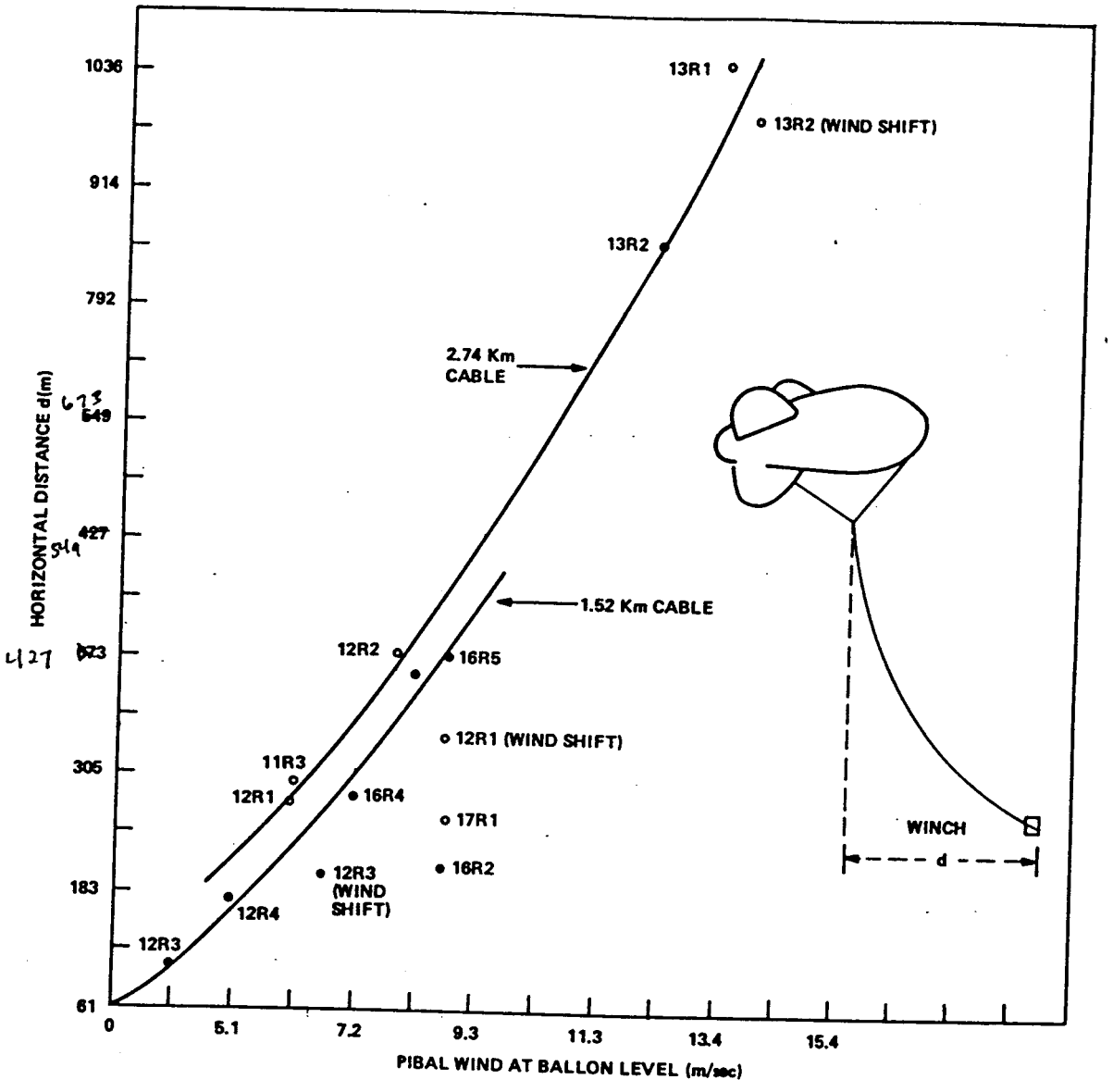

Figure 19. Horizontal Displacement vs Ambient Wind Speed

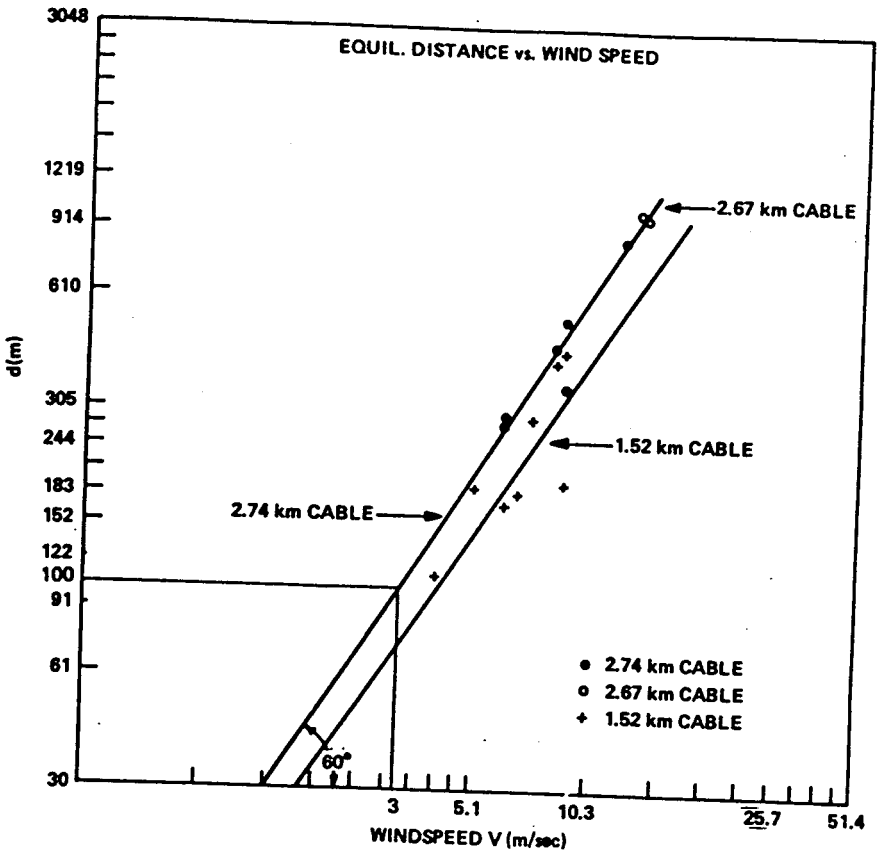

$\ln(d)$ vs. $\ln(V_w)$

FOR 2.74 km CABLE

$$\frac{\ln d - \ln 100}{\ln V - \ln 3} = \tan 60°$$

$$\ln d = 1.7 \ln V - 1.7 \ln 3 + \ln 100$$

$$\ln d = \ln \left[V^{1.7} \times \frac{100}{3^{1.7}} \right]$$

$$d = \frac{100}{3^{1.7}} V^{1.7} = f(L) V^{1.7}$$

Figure 20. Graph: $\ln(d)$ vs $\ln(V_w)$

2.7 Balloon Flight Altitude

2.7.1 ALTITUDE VS DISPLACEMENT

In Figure 21, the average (most frequent value) float altitude is plotted versus horizontal displacement for the flights on the 1.52- and 2.74-km cables.

Despite the somewhat arbitrary choices for values of d, and the fact that each flight experienced a different wind profile along the cable, the data tend to conform quite well to a simple, non-linear relationship between altitude and displacement, d.

2.7.2 RANGE IN ALTITUDE VS WIND SPEED

Figure 22 shows the range in altitude during a 20-min flight versus the ambient wind speed. The balloon flew highest and had least vertical displacement in a 9.3 m/sec wind on the 2.74-km cable (Flight 11R3) and in a wind less than 5.1 m/sec on the 1.52-km cable (Flight 11R4). Although there usually is a wind speed range in which the aerodynamic characteristics of a particular balloon are optimum, these 5.1 - 9.3 m/sec wind speeds are considered too low to produce, for example, a maximum ratio of aerodynamic lift to drag force, and the explanation must lie in other environmental parameters.

2.7.3 EFFECT OF SUPERHEAT AND CABLE DRAG

The flights cited above were made on the same day near noon, so that there might have been useful static lift due to superheat. In each case, the winds along the cable were very light (see Figures 3 and 8), and the anemometer records indicate no strong gusts. The balloon also was very stable, but flying low, in 9.3 m/sec wind during the first part of Flight 16R3 which was flown at 1300 hr when the vertical wind profile was about 10.2 m/sec all along the cable. The cable length was 2.44 km and was subsequently foreshortened to 2.13 km due to some cloudiness near the 2.74 km level.

The cloudiness can account for the fact that on all of the flights on April 16 the balloon was flying low. Cooler lifting gas can cause a decrease in helium volume and hence a decrease in static lift of the balloon. Nevertheless, there was a diurnal effect due to changing superheat. Compare the start times for the "16R" flights, Table 2(a), with the maximum altitudes shown in Figure 22, and note the decrease in altitude with time after noon, particularly Flights 16R2 and 16R5, both at 17 knots, flown at noon and at 1500 hr, respectively.

Increased drag forces due to winds along the cable also tend to lower the altitude. Although the actual vertical wind profile at a given instant during flight is not known, it is reasonable to assume that the PIBAL profile closest in time probably gives a useful indication of the actual profile. The highest altitudes during Runs 16R2 and 16R5 occurred during the earlier portions of the respective

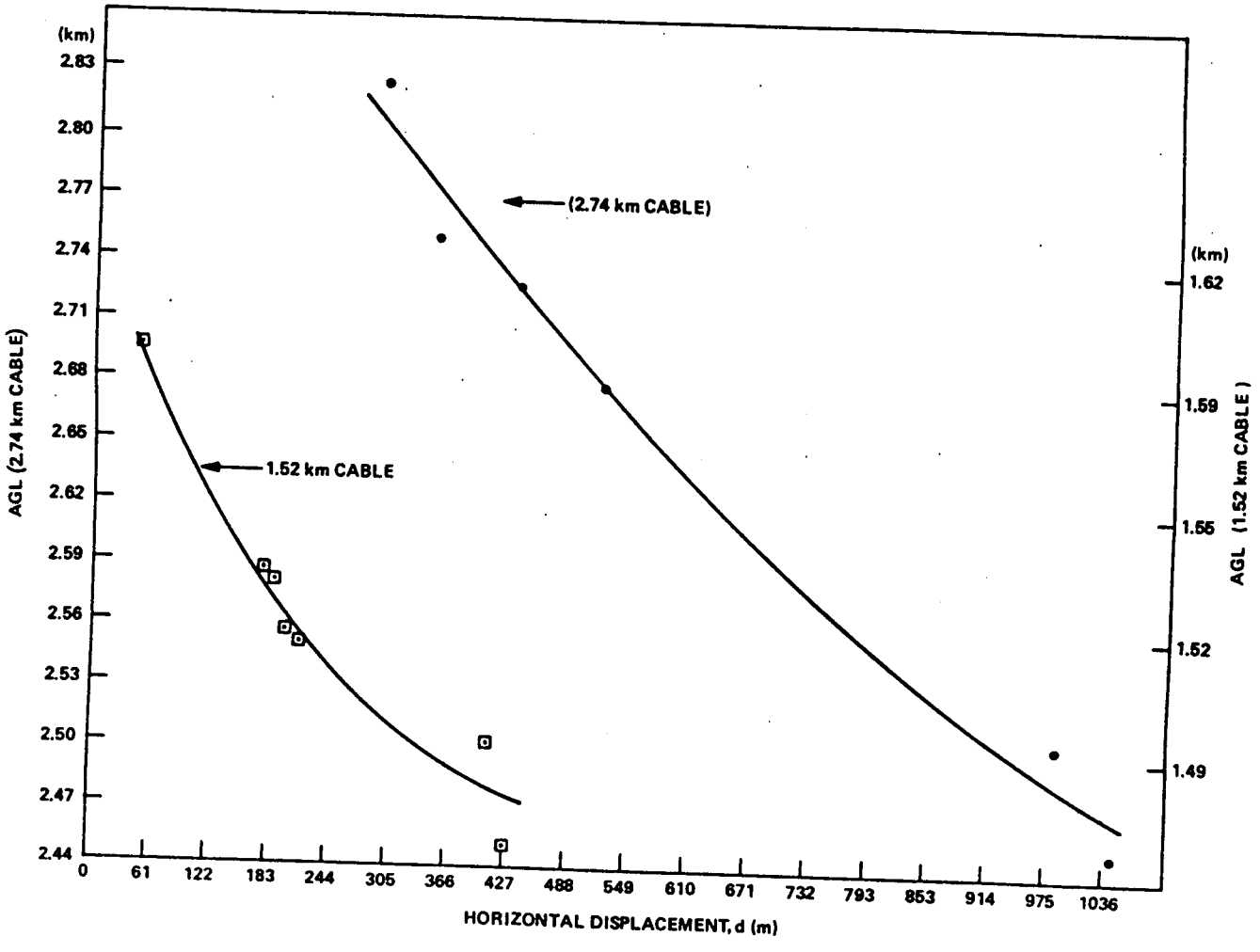

Figure 21. Average Float Altitude vs Horizontal Displacement

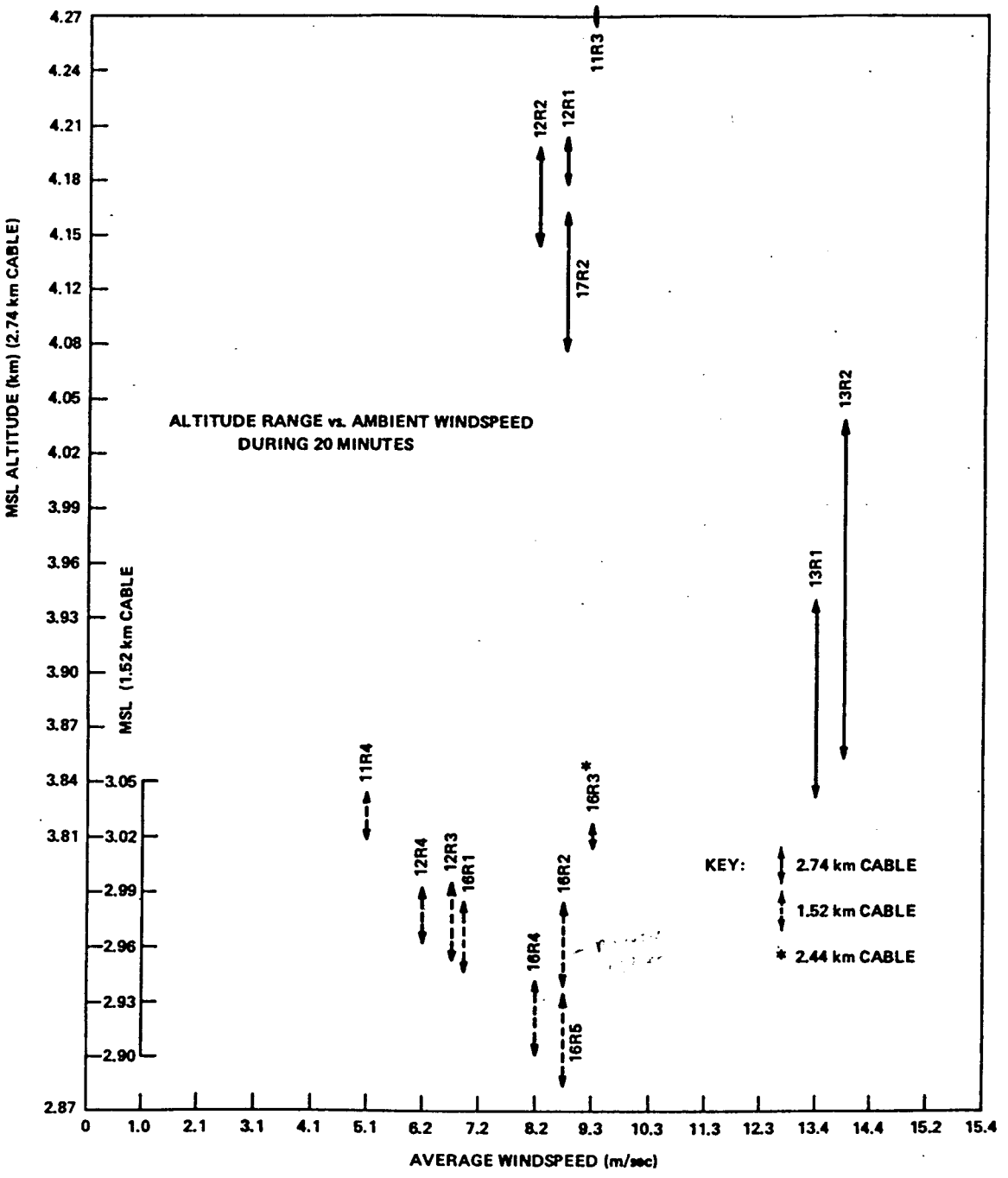

Figure 22. Range in Altitude vs Ambient Wind Speed

flights. From the corresponding PIBAL wind profiles, Figures 10 and 14, it appears that the cable drag forces due to these winds were a little larger in Flight 16R2, the noontime flight, and thus tended to lower the altitude in opposition to the superheat effect.

2.8 Ground Speeds and Accelerations

Each trajectory, however complex, is a continuous succession of 3-dimensional "excursions" in which the balloon speed is low near the extremes, and relatively high at some intermediate point along the path. The low speed generally was 0.3 to 0.6 m/sec. On all of the flights [Tables 1(b), 2(b), and 3(b)] the listed value of maximum speed tangent to the balloon trajectory was considerably higher than the typical peak speed that was reached during most of the excursions during the 20-min test. From the record of speed versus time shown in Figure 16, it is clear that on the more complex trajectories there was no "typical" excursion; in those cases the value listed as typical is the arithmetic average.

Figure 23 shows the maximum ground speed and the maximum relative wind speed recorded during the same flight. (They do not occur, of course, at the

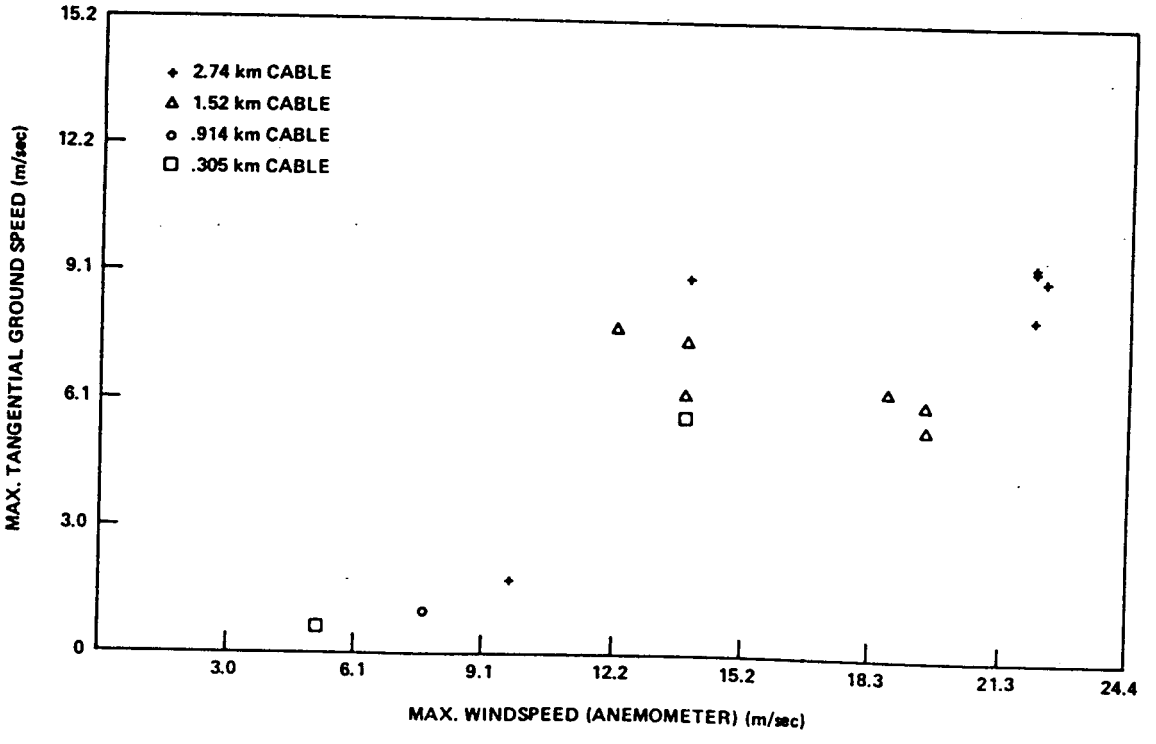

Figure 23. Maximum Ground Speed vs Maximum Relative Wind Speed

same instant.) We have no information concerning the gust impulse which supplied the energy to accelerate the balloon to maximum ground speed; however, for those gusts that were encountered during the tests, the instantaneous balloon speed never exceeded 9.4 m/sec when maximum "wind speed" on an individual flight was 12.2 to 19.5 m/sec. Similarly, on the 1.52-km cable, the maximum balloon speed was limited to 7.9 m/sec when the maximum wind speed was 12.2 to 19.5 m/sec.

On all of the flights the acceleration relative to ground never exceeded 0.1 G ± 0.05 G, (0.10 m/sec^2). In fact, on most flights the most probable value was less than 0.05 G. The acceleration versus time graph shown in Figure 16 is typical of the more complex motions.

2.9 "Wander"

In this report the range of the motion, traditionally called the horizontal wander of the balloon, is arbitrarily defined as the maximum diagonal of the area that includes all points in the horizontal trajectory. The measurements, determined graphically, are listed in Tables 1, 2, and 3.

To illustrate the overall system performance, wander versus ambient wind speed are plotted in Figure 24.

Wander results from gust energy, which has no clear relationship to ambient wind speed. Moreover, wander is affected by gusts acting along the cable as well as on the balloon; therefore, a good correlation between wander and ambient wind speed would be surprising. A better correlation is to be expected between wander and the maximum tangential ground speed of the balloon, since both quantities are the result of gusts (Figure 25).

2.10 Cable Tension at the Confluence Point

Cable tension at the confluence point is the magnitude of the vector which balances the vector sum of (a) the static and aerodynamic lift of the balloon, (b) the weight of the balloon and payload, and (c) the drag force on the balloon.

Since the cable angles and the angles of attack of the balloon are not known, a quantitative interpretation of the data relative to the aerodynamic characteristics of the balloon has not been attempted. The range in values and the typical value of tension for each flight are shown with the ambient wind speed in Figure 26. In most flights the extreme values occurred very infrequently.

2.10.1 TENSION VS SLANT RANGE

Typically, as noted in Section 2.2.2, and shown on Figure 16 for Flight 16R2, extreme values in tension coincided with extremes in slant range, with the maximum tension occurring when the balloon was flying high and close in horizontal

distance to the winch; and minimum tension, when the balloon was flying low, and away from the winch. Highly damped quasiharmonic variations were observed during flights at altitudes considerably below the design altitude of the system.

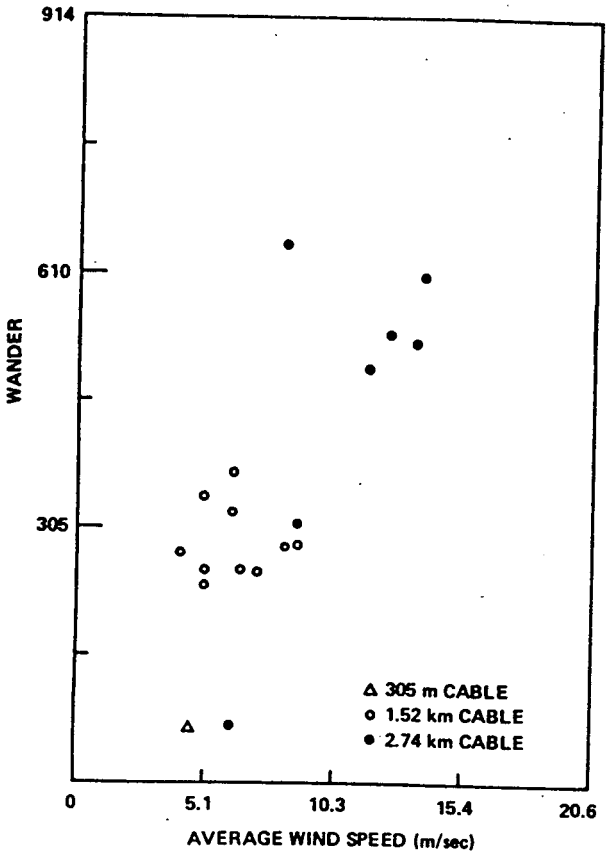

Figure 24. Wander vs Ambient Wind Speed

2. 10. 2 TENSION AND PITCH ANGLE

On all of the flights, when there was a significant, abrupt change in tension, there was a corresponding change in pitch angle of the target box. The increments were not proportional. The pitch angle variations lagged the change in tension by 3 to 4 sec (Figure 17). This has been determined not to be a peculiarity of the instrumentation; it may be a balloon system modal characteristic, or it may be directly due to the cable-payload coupling arrangement (Figure 2).

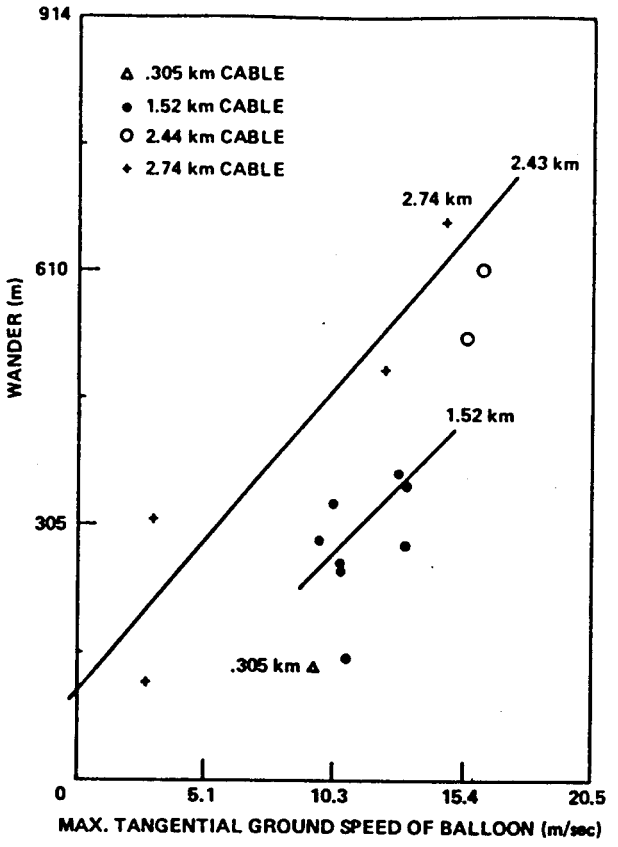

Figure 25. Wander vs Maximum Tangential Groundspeed

2.11 Damping Characteristics

Figures 3 through 7 show three quite different patterns of actual motion using the 2.74-km cable (2.67 km on Flight 13R2). The strong damping evident in the almost linear trajectories (Figures 3 and 4) has already been noted. The flights on the 1.52-km cable (Figures 8 and 9) in particular, also illustrate damping characteristics which enable the system to recover from a single, unusually large, rapid excursion. Other possible modes, of course, may be less highly damped. When successive gusts overlap or if several modes exist simultaneously, the damping becomes masked in the complex response (Figure 6, for example).

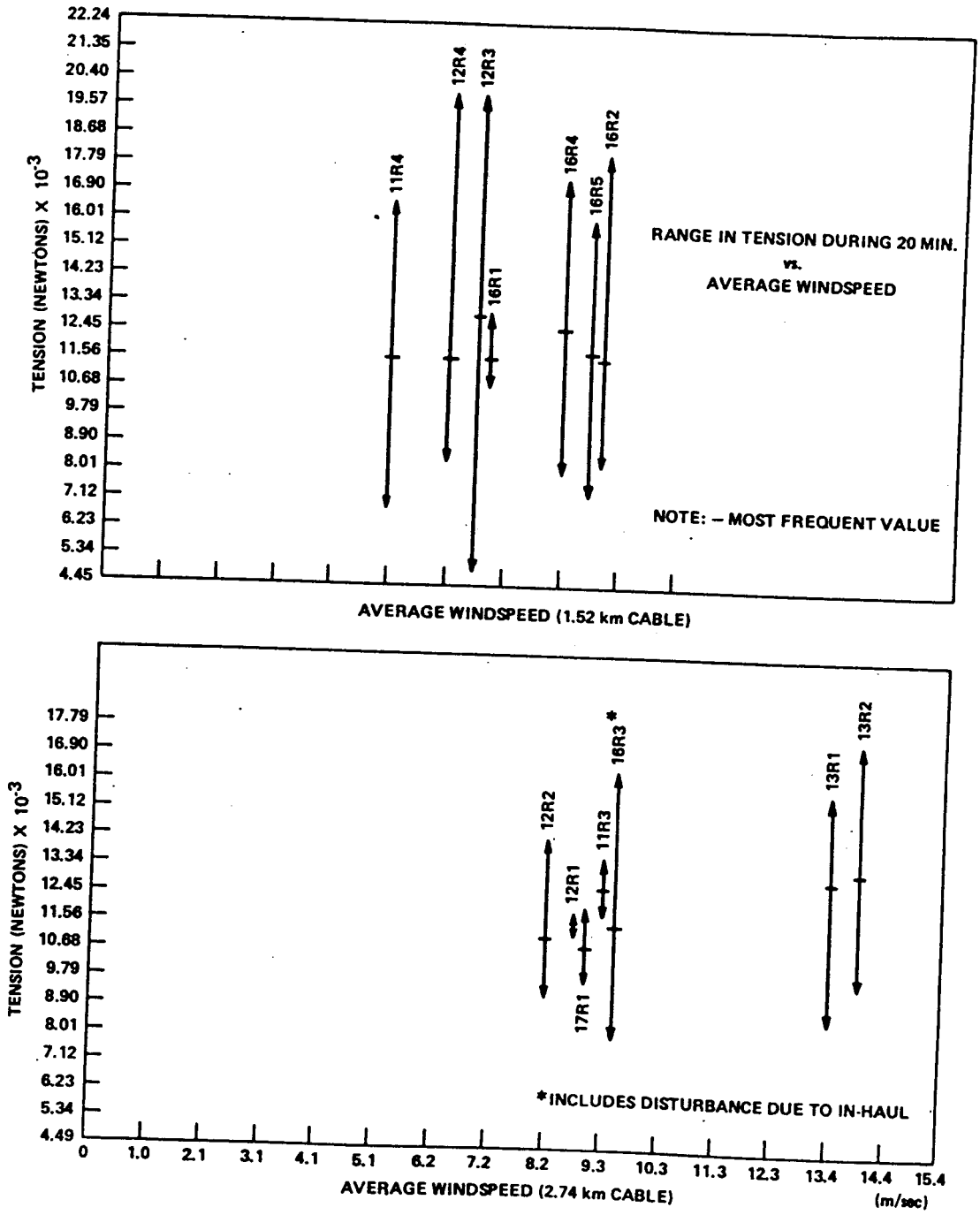

Figure 26. Tension vs Average Wind Speed

3. DISCUSSION

3.1 Pertinent Analytical Studies

It is the essence of the scientific, experimental method that the results of observations should be compared with theoretical predictions and the discrepancies carefully analyzed. Ordinarily, experimental controls are devised so that the test environment conforms closely to the theoretical premises. In this project, however, the experimental endeavor was pragmatic. The problem in reconciling theory and practice is due to the difficulty in devising a reasonably simple, workable theory (model) that adequately describes the experimental environment.

In recent analytical studies of the stability and dynamic behavior of three tethered balloon systems at Goodyear Aerospace Corporation, Doyle, Vorachek, Burbick and Block in 1972 and 1973 developed a set of non-linear differential equations to describe the motion in three dimensions (see Bibliography). The tether line was modelled by three discrete, linear links. By assuming the balloon to be near equilibrium, the equations were linearized and separated into motions parallel and transverse to the wind. The method of Laplace transforms was applied to obtain the characteristic polynomial whose roots identify the natural and damped frequencies and damping ratios of the oscillatory modes, and the decay of the aperiodic modes, for essentially uncoupled orthogonal motions. The dynamics of these motions under the influence of a simulated wind gust were predicted by numerically integrating the linearized equations of motion by digital computer.

The authors also have compared the results of their computerized analyses with the observed motions of a 1.98×10^3 m^3 A-shape balloon after it was displaced either parallel or transverse to the wind (in a simulation of a single gust). The predicted and observed values for frequency of oscillation and mode shape for longitudinal motion were in good agreement, but the displacement values for both directions were not. In real life: (1) the balloon usually is not in quasi-equilibrium and the orthogonal motions are not uncoupled; and (2) the forcing functions, which are essentially the dynamic pressures acting on the balloon and along the entire length of the cable, are gusts for which the individual time of onset, pulse shape and duration, and direction relative to the instantaneous orientation of the balloon are not known.

The analytical approach is invaluable in system design, making it possible to study the effects of specific alterations in balloon shape, type or length of cable, and payload weight, for example. However, it does not yet meet existing operational requirements for measurements of the actual displacements and extent of wander of a tethered platform.

The highly damped, low frequency modal characteristics of the large, A-shape balloon on a long tether which have been demonstrated in these flights are consistent with the predictions of the Goodyear analyses. Those theoretical studies also predict that the system will oscillate as a lightly damped, upside-down simple pendulum when flown at altitudes considerably below the design value. The flights on the 914 m and 305 m cables tend to confirm the pendulum-like motions, but the observed oscillations were quite noticeably damped. The period of a 305 m simple pendulum is 36 sec; the observed period (of the target) was about 56 sec.

3.2 Flight Below Design Altitude

As the flight altitude of an aerodynamic-shape balloon with a ballonet (air chamber) is decreased by shortening the tether length, the ballonet fills with an amount of air equal to the decrease in lifting gas volume. The change in the relative volumes of lifting gas and ballonet air causes the location of the center of mass to change relative to the center of pressure of the balloon. This change introduces unbalanced moments which affect the flight characteristics of the system at altitudes very different from the design altitude.

The single effect of changing the cable length (and altitude level) cannot be isolated in the flight results because the wind fields could not be controlled, nor could the variability of the winds during the various tests be quantitatively described for comparison among the various tests. Nevertheless, it is noted that on the flights using the 2.74 km cable, which is the length for which the system was designed, the least displacements were recorded (Figures 3, 4, and 5) and the maximum speeds during a typical excursion were generally less than on flights in comparable wind speeds on the 1.52 km cable. (See also paragraph 2.4.2.)

4. CONCLUSIONS

(1) Records of the instantaneous displacement, velocity and acceleration relative to ground, speed relative to the instantaneous wind, and cable tension at the confluence point have been obtained for a 2832 m^3 British A-shape balloon on 5/8 in. diam NOLARO cable, flying at altitudes near 2.74 km, 2.44 km, 1.52 km, 914 m and 305 m above ground. (Ground elevation was 1436 m.) This was the primary objective of the experiment.

(2) The least motion was observed during a flight when the balloon was on the 2.74 km cable (the design altitude) and ambient wind was approximately 9.3 m/sec. The maximum acceleration was less than 0.1 G; on a typical excursion from equilibrium the maximum ground speed was 0.61 m/sec. Maximum pitch and roll angles of the payload were less than 1.2 and 1.8 deg, respectively.

(3) In the highest ambient wind encountered on the 2.74 km cable (13.9 m/sec in gusts estimated at 23.1 m/sec), the maximum ground speed of the balloon during the 20-min test was 9.4 m/sec and maximum acceleration, 0.1 G.

(4) On the 1.52 km cable in the highest ambient wind (8.8 m/sec with gusts to 18.5 m/sec), the maximum tangential speed attained was 7.9 m/sec and maximum acceleration 0.1 G. On a typical excursion, the ground speed reached 4.6 m/sec and acceleration was less than 0.1 G.

(5) On the shortest cables, 914 m and 305 m, the system tended to oscillate about its equilibrium position like an inverted, damped, simple pendulum. In moderate winds on the 305 m cable, the cable vibrated longitudinally at approximately 0.2 Hz.

(6) Quantitative interpretations of the data are generally precluded by the inability to describe the time of onset, pulse shape, and duration of the gusts to which the balloon and cable were subjected in the ever-changing real wind fields. Measurements of yaw angle, balloon angle of attack, cable angles at both extremes, and cable tension at the winch would also be required for detailed interpretations of the motion; nevertheless,

(a) For a given length of cable, L, the horizontal distance, d, between the winch and the location above which the balloon tended to hover or wander, is approximately related to the ambient wind speed, V_w, by the expression:

$$d = f(L)\, V_w^{1.7}$$

where f(L) is a lumped parameter determined by air density at float altitude and the aerodynamic and gravitational forces along the cable.

(b) The separate effects of changing superheat and different vertical wind profiles on the cable are discernible on some flights.

(7) The large A-shape balloon on a long cable is overdamped so that it recovers from an unusually high gust in a single excursion.

(8) During flights on the 2.74 km and 1.52 km cable, the predominant mode can be described by resolving the motion into directions parallel and transverse to the ambient wind; thus,

(a) The altitude varied (not proportionally) with horizontal displacements from the tethering winch parallel to the wind, with the highest altitudes nearest the tethering winch. When pitching was detectable, it occurred near both extremes of this longitudinal displacement.

(b) The transverse motion was less highly damped, and rolling was directly associated with this motion, the maximum roll angle coinciding with maximum transverse displacement.

(c) Large increases in cable tension at the confluence point were associated with the highest values of slant range. When the latter occurred, the horizontal distance to the winch was relatively small and the altitude relatively high.

Bibliography

Bennett, R. M., Bland, S. R., and Redd, L. T. (1973) Computer Programs for Calculating and Plotting the Stability Characteristics of a Balloon Tethered in a Wind, NASA TM X-2740.

DeLaurier, J. D. (1970) A First Order Theory for Predicting the Stability of Cable Towed and Tethered Bodies Where the Cable Has a General Curvature and Tension Variation, Von Karman Inst. TN-68.

DeLaurier, J. D. (1972) A Stability Analysis of Cable-Body Systems Totally Immersed in a Fluid Stream, NASA CR-2021.

DeLaurier, J. D. (1972) A stability analysis for tethered aerodynamically shaped balloons, J. Aircraft 9(No. 9):646-651.

DeLaurier, J. D. (1974) An Experimental Investigation of the Dynamic Stability of the Family II Balloon, Proceedings, Eighth AFCRL Scientific Balloon Symposium, AFCRL-TR-74-0393.

Doyle, G. R. Jr., and Vorachek, J. J. (1971) Investigation of Stability Characteristics of Tethered Balloon Systems, AD731570.

Doyle, G. R. Jr., Vorachek, J. J., and Block, D. B. (1973) Stability and Dynamic Behavior of Two Tethered Balloon Systems, AFCRL-TR-0396.

Hoerner, S. R. (1958) Fluid-Dynamic Drag, published by the author.

Leclaire, R. C., and Rice, C. B. (1973) The Local Motions of a Payload Supported by a Tritethered Natural Shape Balloon, AFCRL-TR-73-0748.

Leclaire, R. C., and Schumacher, H. L. Jr. (1974) Local Motions of a Payload Supported by a NOLARO Tritethered Balloon, Proceedings, Eighth AFCRL Scientific Balloon Symposium, AFCRL-TR-74-0393.

Peters, P. A., Lysons, H. H., and Shindo, S. (1973) Aerodynamic Coefficients of Four Balloon Shapes at High Attack Angles, Proceedings, Seventh AFCRL Scientific Balloon Symposium, AFCRL-TR-73-0071.

Pohl, R. A., and Odney, K. D. (1973) Tethered and Cable-Powered Heavy Lift Balloon Systems Design, Operations and Applications, Proceedings, Seventh AFCRL Scientific Balloon Symposium, AFCRL-TR-73-0071.

Potter, R. C. (1965) The Stability of Captive Balloons for Instrument Flying, Including Analysis of Multi-Cable Configurations, N67 11729.

Redd, L. T. (1970) A Towing Technique for Determining the Aerodynamic Forces on Tethered Balloons, Proceedings, Sixth AFCRL Scientific Balloon Symposium, AD717149.

Redd, L. T., Bennett, R. M., and Bland, S. R. (1972) Analytical and Experimental Investigation of the Stability of a Balloon Tethered in a Wind, Proceedings Seventh AFCRL Scientif Balloon Symposium, AFCRL-TR-73-0071.

Redd, L. T., Bennett, R. M., and Bland, S. R. (1973) Experimental and Analytical Determination of Stability Parameters for a Balloon Tethered in a Wind, NASA TN F-7222.

Redd, L. T., Bland, S. R., and Bennett, R. M. (1973) Stability Analysis and Trend Study of a Balloon Tethered in a Wind, With Experimental Comparisons, NASA TN-7272.

Vorachek, J. J., Burbick, J. W., and Doyle, G. R. Jr. (1972) Investigation of Dynamic Behavior of Tethered Balloon Systems, AD740723.

Vorachek, J. J., and Doyle, G. R. Jr. (1973) Comparison of Analytically and Experimentally Determined Dynamic Behavior of Tethered Balloons, AFCRL-TR-0284.

Waters, M. H. L. (1959) Some Observations on the Wander of a Kite Balloon, Royal Aircraft Establishment TN Mech Eng 305.

Appendix A

Table A1. 2.83×10^3 m^3 Kite Balloon (See Figure A1)

Maximum Capacity of Envelope	2.83×10^3 m^3
Maximum Volume of Air-Filled Tail	243 m^3
Maximum Diameter of Envelope	13.2 m
Length of Envelope	36.6 m
Overall Width with Fins Inflated	14.6 m
Overall Height from Bottom of Rudder	16.2 m
Height of Balloon from Rigging Confluence Point	22.3 m
Ballonet Capacity	To permit a flying altitude of 4.57 km
Weight with Accessories Less Cable	8.1×10^3 N

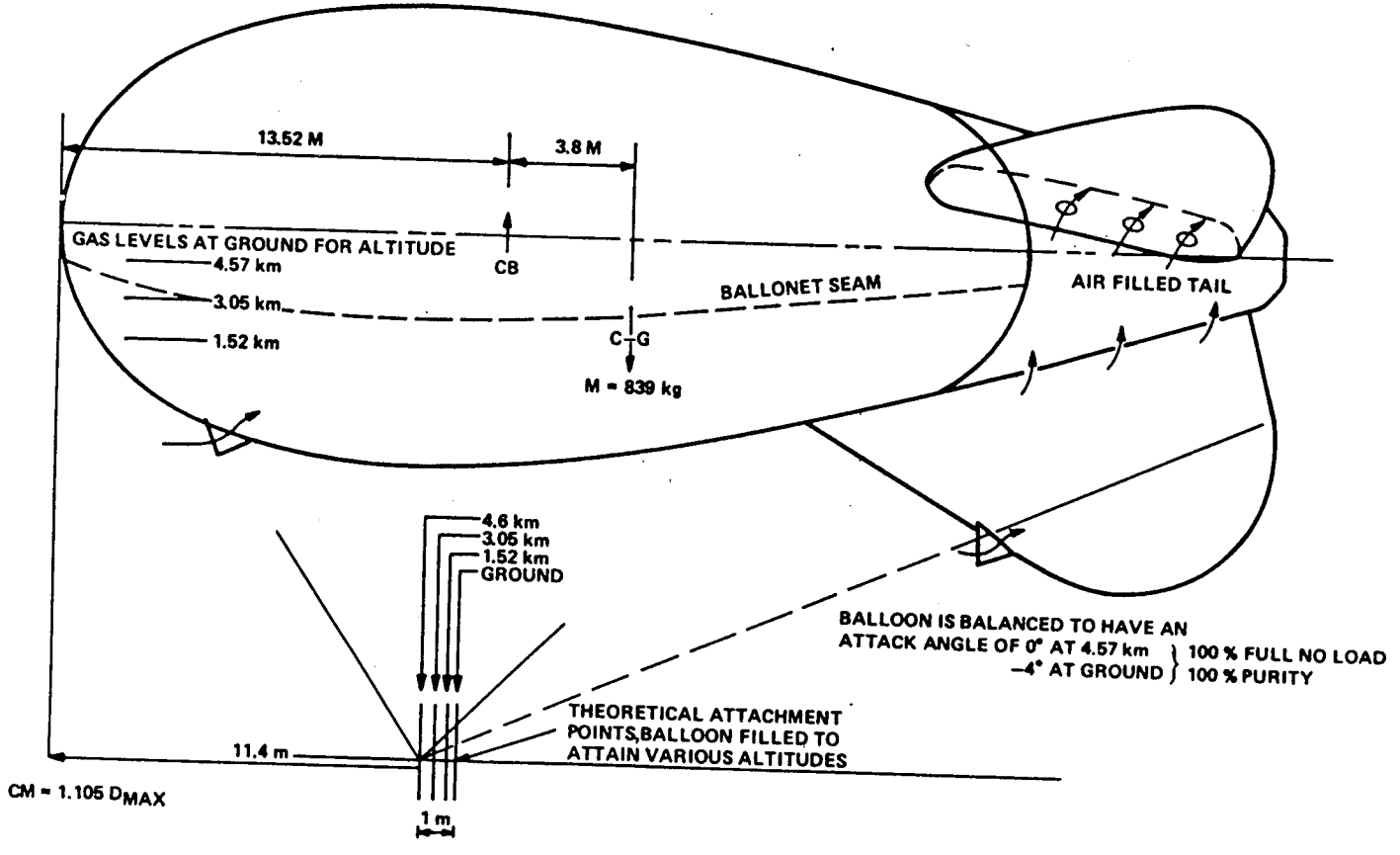

Figure A1. Position of CG, CB, Rigging Confluence Point, 2.83×10^3 m^3 Balloon